Article

Cell Host & Microbe

Depletion of Butyrate-Producing *Clostridia* from the Gut Microbiota Drives an Aerobic Luminal Expansion of *Salmonella*

Graphical Abstract

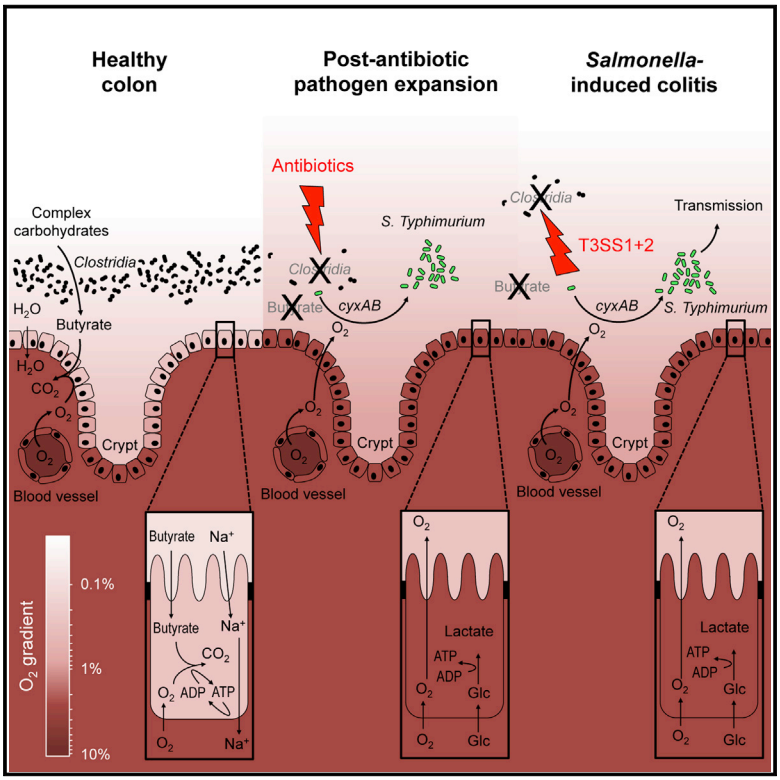

Highlights

- *Salmonella*-induced colitis drives a depletion of butyrate-producing *Clostridia*
- Antibiotic-mediated depletion of *Clostridia* increases colonocyte oxygenation
- Increased epithelial oxygenation drives an aerobic post-antibiotic pathogen expansion
- A respiration-driven *Salmonella* expansion in the gut is required for transmission

Authors

Fabian Rivera-Chávez, Lillian F. Zhang, Franziska Faber, ..., Carlito B. Lebrilla, Sebastian E. Winter, Andreas J. Bäumler

Correspondence

ajbaumler@ucdavis.edu

In Brief

Paradoxically, antibiotic treatment can promote relapse of *Salmonella* gastroenteritis. Rivera-Chávez et al. show that antibiotic treatment lowers colonization resistance by depleting butyrate-producing *Clostridia*. Decreased butyrate availability increases epithelial oxygenation, thereby fueling aerobic pathogen expansion in the gut lumen. Aerobic respiration synergizes with nitrate respiration to drive fecal-oral transmission of *Salmonella*.

Rivera-Chávez et al., 2016, Cell Host & Microbe *19*, 443–454
April 13, 2016
http://dx.doi.org/10.1016/j.chom.2016.03.004

Cell Host & Microbe
Article

Depletion of Butyrate-Producing *Clostridia* from the Gut Microbiota Drives an Aerobic Luminal Expansion of *Salmonella*

Fabian Rivera-Chávez,[1] Lillian F. Zhang,[1] Franziska Faber,[1] Christopher A. Lopez,[1] Mariana X. Byndloss,[1] Erin E. Olsan,[1] Gege Xu,[2] Eric M. Velazquez,[1] Carlito B. Lebrilla,[2] Sebastian E. Winter,[3] and Andreas J. Bäumler[1,*]
[1]Department of Medical Microbiology and Immunology, School of Medicine, University of California at Davis, One Shields Avenue, Davis, CA 95616, USA
[2]Department of Chemistry, College of Letters and Sciences, University of California at Davis, One Shields Avenue, Davis, CA 95616, USA
[3]Department of Microbiology, University of Texas Southwestern Medical Center, 5323 Harry Hines Boulevard, Dallas, TX 75390, USA
*Correspondence: ajbaumler@ucdavis.edu
http://dx.doi.org/10.1016/j.chom.2016.03.004

SUMMARY

The mammalian intestine is host to a microbial community that prevents pathogen expansion through unknown mechanisms, while antibiotic treatment can increase susceptibility to enteric pathogens. Here we show that streptomycin treatment depleted commensal, butyrate-producing *Clostridia* from the mouse intestinal lumen, leading to decreased butyrate levels, increased epithelial oxygenation, and aerobic expansion of *Salmonella enterica* serovar Typhimurium. Epithelial hypoxia and *Salmonella* restriction could be restored by tributyrin treatment. *Clostridia* depletion and aerobic *Salmonella* expansion were also observed in the absence of streptomycin treatment in genetically resistant mice but proceeded with slower kinetics and required the presence of functional *Salmonella* type III secretion systems. The *Salmonella* cytochrome *bd*-II oxidase synergized with nitrate reductases to drive luminal expansion, and both were required for fecal-oral transmission. We conclude that *Salmonella* virulence factors and antibiotic treatment promote pathogen expansion through the same mechanism: depletion of butyrate-producing *Clostridia* to elevate epithelial oxygenation, allowing aerobic *Salmonella* growth.

INTRODUCTION

Non-typhoidal *Salmonella enterica* serovars, such as *S. enterica* serovar Typhimurium (*S.* Typhimurium), are a common cause of human gastroenteritis (Majowicz et al., 2010). Studies using animal models of infection show that upon ingestion, *S.* Typhimurium uses the invasion-associated type III secretion system (T3SS-1) to enter intestinal epithelial cells (Galán and Curtiss, 1989). After crossing the epithelial barrier, the pathogen deploys a second type III secretion system (T3SS-2) to enhance its survival in the underlying tissue (Hensel et al., 1995). T3SS-1-mediated epithelial invasion and T3SS-2-mediated survival in tissue trigger acute intestinal inflammation and diarrhea (Tsolis et al., 1999), the hallmarks of gastroenteritis. Interestingly, intestinal inflammation confers a benefit to the pathogen because it drives its expansion in the lumen of the large bowel (Barman et al., 2008; Stecher et al., 2007), which is required for fecal-oral transmission of *S.* Typhimurium to the next susceptible host (Lawley et al., 2008).

One mechanism that powers a luminal expansion of *S.* Typhimurium during colitis is the generation of respiratory electron acceptors as a by-product of the inflammatory host response (Ali et al., 2014; Lopez et al., 2015, 2012; Rivera-Chávez et al., 2013; Thiennimitr et al., 2011; Winter et al., 2010). For example, reactive nitrogen species generated by the inflammatory host response can react to form nitrate, the preferred respiratory electron acceptor of *S.* Typhimurium under anaerobiosis (Lopez et al., 2015, 2012).

A history of antibiotic usage is a risk factor for developing *S. enterica*-induced gastroenteritis (Pavia et al., 1990), and antibiotic treatment during convalescence may on occasion produce a bacteriologic and symptomatic relapse (Aserkoff and Bennett, 1969; Nelson et al., 1980). These effects of antibiotics can be modeled in mice, as treatment with streptomycin leads to a marked expansion of *S.* Typhimurium in the lumen of the murine large intestine (Que and Hentges, 1985). The mechanisms contributing to this post-antibiotic pathogen expansion remain poorly understood.

Antibiotic treatment increases epithelial oxygenation in the large intestine (Kelly et al., 2015), which is predicted to elevate diffusion of oxygen into the gut lumen (Espey, 2013). Oxygen is the only respiratory electron acceptor with a higher redox potential than nitrate. Work on oxygen respiration in *Escherichia coli* suggests that under conditions of high aeration, *S.* Typhimurium predominantly uses the low-affinity cytochrome bo_3 oxidase encoded by *cyoAB* (Alexeeva et al., 2003; Cotter et al., 1990; Cotter et al., 1992; Cotter and Gunsalus, 1992; Fu et al., 1991). When the pathogen enters host tissue, it encounters an oxygen partial pressure (pO_2) of 23–70 mmHg (3%–10% oxygen), which is considerably lower than the atmospheric pO_2 of 160 mmHg (21% O_2) (Carreau et al., 2011). *S.* Typhimurium relies on the high-affinity cytochrome *bd* oxidase encoded by the *cydAB* genes to support its growth in tissue during infection of mice (Craig et al., 2013).

Importantly, the *S.* Typhimurium chromosome encodes another enzyme with homology to cytochrome *bd* oxidase. This enzyme is termed cytochrome *bd*-II oxidase and is encoded by the *S.* Typhimurium *cyxAB* operon (Atlung and Brøndsted, 1994; Dassa et al., 1991; McClelland et al., 2001). Cytochrome *bd*-II oxidase remains poorly characterized, and its physiological role is not known. Regulation of the *cyxAB* operon in *E. coli* suggests that cytochrome *bd*-II oxidase might have a function under even more oxygen-limiting conditions than cytochrome *bd* oxidase (Brøndsted and Atlung, 1996), but this hypothesis has not been tested. Here we investigated whether cytochrome *bd*-II oxidase contributes to expansion of *S.* Typhimurium in the large intestine.

RESULTS

Cytochrome *bd* and *bd*-II Oxidases Are Required for Growth in Different Host Niches

We generated *S.* Typhimurium mutants lacking either a functional cytochrome *bd* oxidase (*cydA* mutant) or a functional cytochrome *bd*-II oxidase (*cyxA* mutant) to investigate how aerobic respiration affects growth of the pathogen. The *S.* Typhimurium wild-type exhibited a fitness advantage over the *cydA* mutant during growth with 8% oxygen, which corresponds to tissue oxygenation (3%–10% oxygen). However, the *cydA* gene did not confer a fitness advantage during growth with 0.8% oxygen (Figure 1A), which was consistent with repression of the *E. coli cydAB* operon in low-oxygen environments (Tseng et al., 1996). The *cyxA* gene was not required for growth with 8% oxygen or with 0% oxygen but provided a fitness advantage during growth with 0.8% oxygen (Figure 1B).

To assess the contribution of *cydA* and *cyxA* to growth in host tissue, mice (C57BL/6) were infected intraperitoneally with a 1:1 mixture of the wild-type and the *cydA* mutant or a 1:1 mixture of the wild-type and the *cyxA* mutant, respectively (competitive infection). 4 days after infection, the wild-type was recovered in significantly higher numbers from the spleen than the *cydA* mutant (Figure 1C), confirming that cytochrome *bd* oxidase contributes to growth in tissue (Craig et al., 2013). In contrast, *cyxA* was dispensable for growth in tissue.

We next investigated the contribution of *cydA* and *cyxA* to post-antibiotic pathogen expansion in the colon contents of mice. To this end, mice (C57BL/6) received a single dose of streptomycin intragastrically and were infected 1 day later with a 1:1 mixture of the wild-type and the *cydA* mutant or a 1:1 mixture of the wild-type and the *cyxA* mutant. 4 days after infection, the *cydA* gene was dispensable for post-antibiotic pathogen expansion, while the *cyxA* gene conferred a significant ($p < 0.05$) fitness advantage (Figure 1D). Importantly, the *cyxA* mutant did not confer a fitness advantage in the colon of mice that had not received antibiotics, suggesting that cytochrome *bd*-II oxidase contributed to post-antibiotic pathogen expansion in the gut (Figure 1D).

Collectively, our data indicated that *cydA* was exclusively required during growth in host tissue (Figure 1C), while *cyxA* contributed exclusively to growth under the more oxygen-limited conditions encountered in the antibiotic-treated gut (Figure 1D).

Cytochrome *bd*-II Oxidase and Nitrate Reductases Synergistically Drive Post-antibiotic Pathogen Expansion

Consistent with previous studies suggesting that nitrate respiration contributes to a post-antibiotic pathogen expansion (Lopez et al., 2015, 2012), the *S.* Typhimurium wild-type was recovered in approximately 8-fold higher numbers than a nitrate respiration-deficient mutant (*narG napA narZ* mutant) 4 days after competitive infection of streptomycin-treated mice (C57BL/6) (Figure 1E). To investigate whether nitrate respiration and aerobic respiration cooperated during post-antibiotic pathogen expansion, we constructed a *cyxA narG napA narZ* mutant and compared its fitness with that of wild-type *S.* Typhimurium. Recovery of bacteria 4 days after infection revealed a remarkable synergy between nitrate respiration and aerobic respiration, as the wild-type was recovered in approximately 2,000-fold higher numbers than the respiration-deficient *cyxA narG napA narZ* mutant (Figures 1E and S1A). Importantly, the *S.* Typhimurium wild-type and *cyxA narG napA narZ* mutant were recovered in similar numbers from mice that had not received streptomycin, suggesting that nitrate respiration and aerobic respiration cooperated during post-antibiotic pathogen expansion. Similar results were observed when streptomycin-treated mice were infected with individual *S.* Typhimurium strains (Figure 1F).

Cytochrome *bd*-II Oxidase-Dependent Aerobic Growth Is Driven by an Antibiotic-Mediated Depletion of *Clostridia*

The finding that *cyxA* only conferred a growth advantage upon *S.* Typhimurium in streptomycin-treated mice suggested that aerobic pathogen expansion required depletion of a component of the gut-associated microbial community (gut microbiota). Analysis of DNA isolated from feces by quantitative real-time PCR with class-specific primers suggested that streptomycin treatment caused a marked depletion of members of the class *Clostridia* from the gut microbiota within a day (Figure 1G) (Sekirov et al., 2008). By 5 days after streptomycin treatment, the *Clostridia* population had recovered to levels observed prior to antibiotic treatment. *Clostridia* are credited for producing the lion's share of the short-chain fatty acid butyrate, an important fermentation product produced by the gut microbiota (Louis and Flint, 2009; Vital et al., 2014). Cecal butyrate concentrations were diminished by four orders of magnitude 1 day after treatment with streptomycin (Figure 1H). In contrast, streptomycin treatment lowered the concentrations of acetate and propionate in the cecal contents by only one or two orders of magnitude, respectively (Figures S1B and S1C).

We next tested the hypothesis that antibiotic-mediated depletion of *Clostridia* was responsible for an aerobic post-antibiotic pathogen expansion. To this end, streptomycin-treated mice (C57BL/6) were infected with the wild-type and a *cyxA* mutant and inoculated 1 day later with chloroform-treated cecal contents of treatment-naive mice. Since chloroform kills vegetative bacterial cells but not spores, this treatment enriches for *Clostridia*, the dominant group of spore-forming bacteria present in cecal contents (Itoh and Freter, 1989). Inoculation of streptomycin-treated mice with chloroform-treated cecal contents

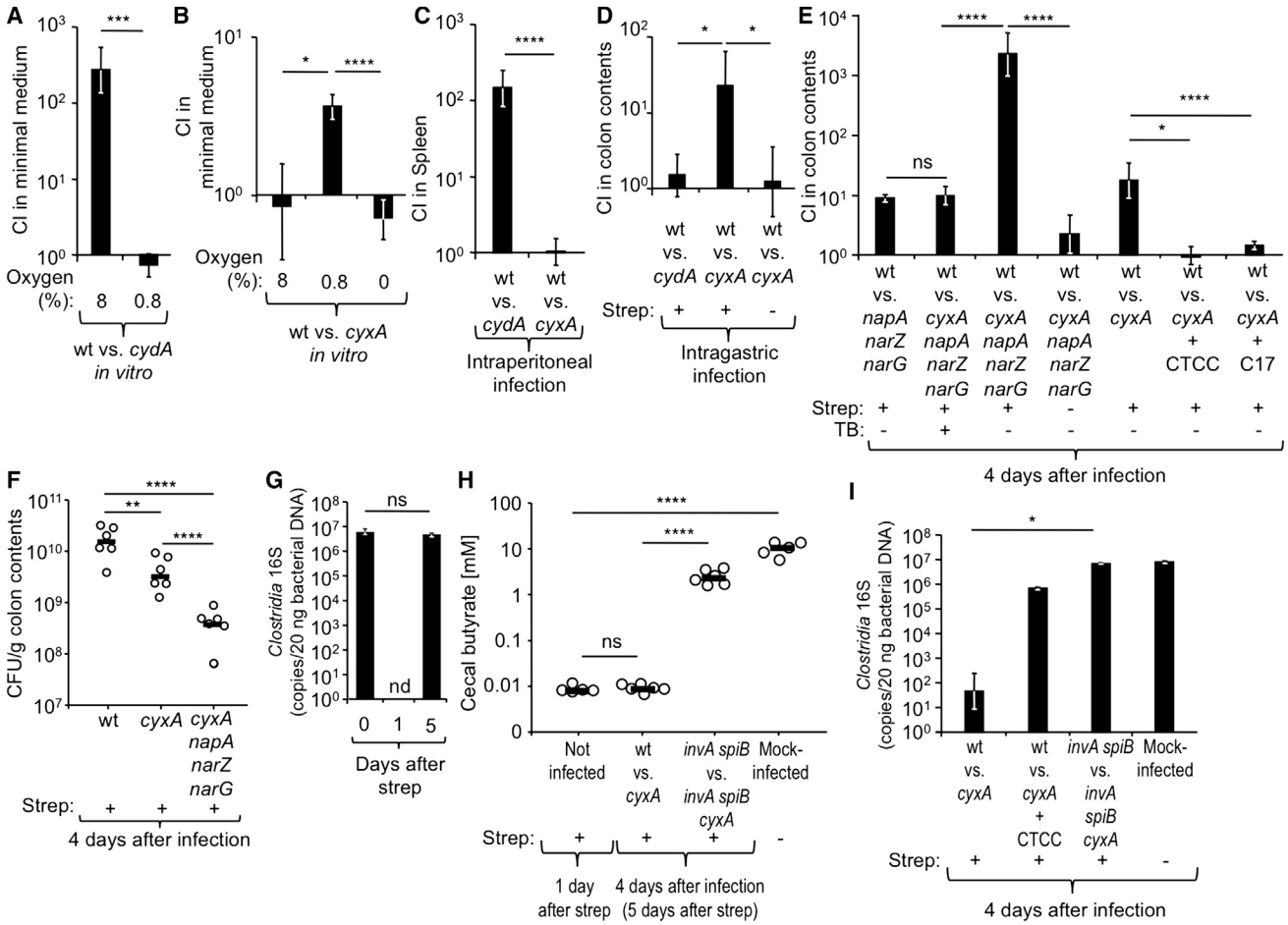

Figure 1. Cytochrome *bd*-II Oxidase Contributes to Post-antibiotic Pathogen Expansion

(A and B) Minimal medium was inoculated with the indicated strains, and the competitive index (CI) was determined after 24 hr incubation in the presence of 8%, 0.8%, or 0% oxygen.

(C) Groups of C57BL/6 mice (n = 4) were infected intraperitoneally with the indicated strain mixtures, and the CI was determined 4 days after infection.

(D) The CI in colon contents was determined 4 days after infection.

(E) 2 days after infection, some mice were inoculated intragastrically with a culture of 17 human *Clostridia* isolates (C17). For tributyrin (TB) supplementation mice received TB 4 hr prior to infection and 2 days after infection, and the CI was determined 4 days after infection. For (E) and (I), 1 day after infection, some mice received chloroform-treated cecal contents (CTCC) of treatment-naive mice intragastrically.

(F) CFU recovered from colon contents 4 days after infection with individual *S*. Typhimurium strains. For (F) and (H), each circle represents data from an individual animal.

(G) *Clostridia* 16S rRNA gene copy numbers present in 20 ng of total bacterial DNA were determined at the indicated time points.

(H) The concentration of butyrate was measured in cecal contents at the indicated time points after streptomycin treatment (see also Figures S1B and S1C).

(I) *Clostridia* 16S rRNA gene copy numbers present in 20 ng of total bacterial DNA were determined.

Bars represent geometric means ± SE. *p < 0.05; **p < 0.01; ***p < 0.005; ****p < 0.001; ns, not statistically significantly different; nd, none detected; wt, *S*. Typhimurium wild-type.

increased the abundance of *Clostridia* (Figure 1I) and annulled the fitness advantage conferred by cytochrome *bd*-II oxidase (Figure 1E).

To directly test whether *Clostridia* depletion was responsible for driving an aerobic *S.* Typhimurium expansion, streptomycin-treated mice were infected with the wild-type and a *cyxA* mutant and inoculated 2 days later with a community of 17 human *Clostridia* isolates (Atarashi et al., 2013, 2011; Narushima et al., 2014). Remarkably, inoculation with the 17 human *Clostridia* isolates abrogated the fitness advantage conferred by the *cyxA* gene (Figures 1E and S1A).

Clostridia Depletion Increases Oxygenation of Colonocytes to Drive a Cytochrome *bd*-II Oxidase-Dependent Aerobic Pathogen Expansion

We next wanted to investigate how the prevalence of *Clostridia* could alter oxygen availability in the gut. *Clostridia* are the main producers of butyrate (Louis and Flint, 2009; Vital et al., 2014), which serves as the preferred energy source for colonocytes (enterocytes of the colon). Colonocytes oxidize butyrate to carbon dioxide (CO_2) (Donohoe et al., 2012), thereby rendering the epithelium hypoxic (<7.6 mmHg or <1% O_2) (Kelly et al., 2015). However, in germ-free mice, where butyrate is absent,

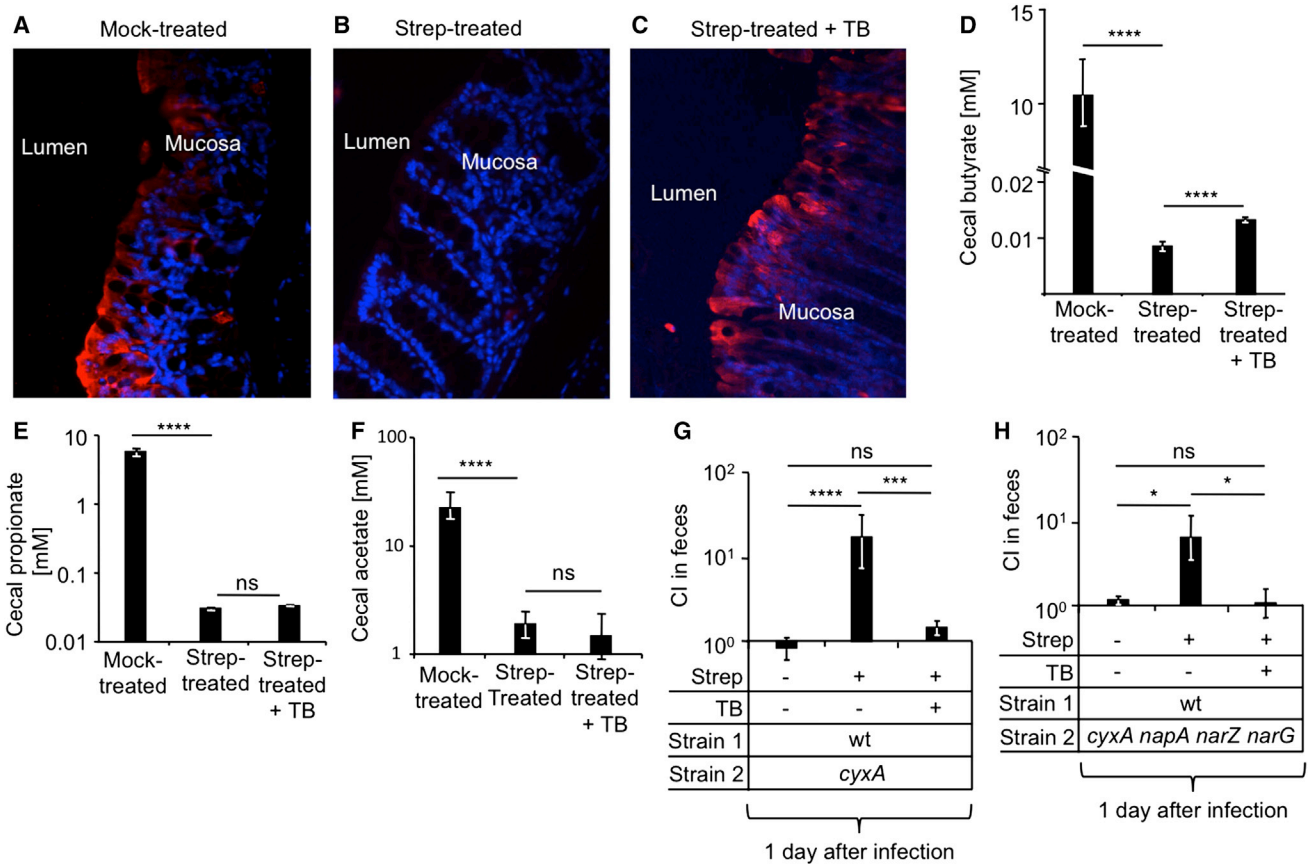

Figure 2. Tributyrin Treatment Restores Physiologic Hypoxia of Colonocytes and Prevents Cytochrome *bd*-II Oxidase-Dependent Post-antibiotic Pathogen Expansion

(A–C) Groups of C57BL/6 mice (n = 4) were mock treated (A), treated with streptomycin (Strep) (B), or treated with streptomycin and tributyrin (TB) (C), and the colon was collected 1 day later. Binding of pimonidazole (red fluorescence) was detected in sections of the colon counter-stained with DAPI nuclear stain (blue fluorescence). Representative images are shown.

(D–F) Groups of C57BL/6 mice (n = 5) were mock treated, treated with streptomycin, or treated with streptomycin and TB. Concentrations of butyrate (D), propionate (E), and acetate (F) in cecal contents were determined 8 hr after TB supplementation.

(G and H) Groups of C57BL/6 mice (n is shown in Figure S1A, except for TB supplementation where n = 4) were mock treated or treated with streptomycin and infected 1 day later with the indicated strain mixtures. Some mice received mock supplementation or were supplemented with tributyrin 8 hr prior to pimonidazole injection. 1 day after infection, the competitive index (CI) in colon contents was determined.

Bars represent geometric means ± SE. *$p < 0.05$; ***$p < 0.005$; ****$p < 0.001$; ns, not statistically significantly different; wt, *S.* Typhimurium wild-type.

colonocytes obtain energy by fermenting glucose to lactate (Donohoe et al., 2012), which is accompanied by an increased oxygenation of the epithelium (Kelly et al., 2015). Since increased oxygenation of the epithelium is predicted to elevate oxygen diffusion into the gut lumen (Espey, 2013), we hypothesized that a depletion of *Clostridia*-derived butyrate would increase the oxygenation of colonocytes and increase diffusion of oxygen into the gut lumen to fuel a *cyxA*-dependent *S.* Typhimurium expansion.

To test this hypothesis, we first investigated whether an antibiotic-mediated depletion of butyrate-producing *Clostridia* would elevate the oxygenation of colonocytes by using the exogenous hypoxia marker pimonidazole. Under hypoxic conditions, nitroreductase enzymes reduce pimonidazole to hydroxylamine intermediates, which bind irreversibly to nucleophilic groups in proteins or DNA (Kizaka-Kondoh and Konse-Nagasawa, 2009). Colonocytes of conventional mice (C57BL/6) exhibited hypoxia as indicated by pimonidazole staining (Figure 2A) (Colgan and Taylor, 2010; Kelly et al., 2015). Streptomycin treatment eliminated staining of colonocytes with pimonidazole (Figure 2B), indicative of a marked increase in colonocyte oxygenation. Next, we supplemented streptomycin-treated mice with 1,2,3-tributyrylglycerol (tributyrin), a food additive (butter flavoring) that exhibits delayed absorption in the proximal gut compared to butyrate, which renders it more effective for increasing butyrate concentrations in the large intestine (Kelly et al., 2015). Remarkably, tributyrin supplementation restored epithelial hypoxia in streptomycin-treated mice (Figure 2C) and significantly ($p < 0.001$) increased the concentration of cecal butyrate (Figure 2D), while the concentrations of propionate and acetate remained unchanged (Figures 2E and 2F). Thus, a streptomycin-mediated depletion of *Clostridia*-derived butyrate increased colonocyte oxygenation.

Since streptomycin treatment resulted in depletion of *Clostridia* and increased oxygenation of colonocytes within 1 day, we

hypothesized that a *cyxA*-dependent fitness advantage might already be apparent at early time points after antibiotic treatment. A significant ($p < 0.05$) fitness advantage conferred by the *cyxA* gene was apparent just 1 day after infection of streptomycin-treated mice; however, no fitness advantage was observed in the absence of streptomycin treatment (Figure 2G). Remarkably, tributyrin supplementation abrogated the fitness advantage conferred by the *cyxA* gene in streptomycin-treated mice (Figure 2G). Similar results were obtained with a *cyxA narG napA narZ* mutant (Figure 2H). Since a benefit of nitrate respiration is not observed 1 day after *S.* Typhimurium infection of streptomycin-treated mice (Lopez et al., 2015), these results point to *cyxA* as the main factor driving an early post-antibiotic expansion of *S.* Typhimurium in the lumen (i.e., 1 day after infection).

At 4 days after infection of streptomycin-treated mice, tributyrin supplementation reduced the fitness advantage conferred by the *cyxA napA narZ narG* genes to that conferred by the *napA narZ narG* genes in the absence of tributyrin supplementation (Figure 1E). This outcome was consistent with the idea that tributyrin supplementation only reduced the fitness advantage conferred by *cyxA*.

T3SS-1 and T3SS-2 Drive a Cytochrome *bd*-II Oxidase-Mediated Aerobic Growth at Later Stages of Infection

To investigate whether virulence factors were required to support luminal growth by aerobic respiration, T3SS-1 and T3SS-2 were inactivated using mutations in the *invA* and *spiB* genes, respectively. Similar to what was observed in the wild-type background, a fitness advantage of the avirulent *invA spiB* mutant over the *invA spiB cyxA* mutant was observed after 1 day of infection in the fecal contents of streptomycin-treated mice (C57BL/6), but not in mice that had not received antibiotics (Figures 3A and S1A). Thus, virulence factors were not required for cytochrome *bd*-II oxidase-mediated growth 1 day after infection (corresponding to 2 days after streptomycin treatment). By 4 days after infection with virulent *S.* Typhimurium strains (i.e., a mixture of wild-type and *cyxA* mutant), mice developed acute inflammation in the cecal mucosa, while no marked inflammatory changes were observed in mice infected with avirulent *S.* Typhimurium strains (i.e., a mixture of *invA spiB* mutant and *invA spiB cyxA* mutant) (Figures 3B, 3C, and S2). Interestingly, while the virulent *S.* Typhimurium wild-type exhibited a fitness advantage over a *cyxA* mutant in colon contents 4 days after infection (corresponding to 5 days after streptomycin treatment), no fitness advantage was observed at this time point when streptomycin-treated mice were inoculated with a 1:1 mixture of the avirulent *invA spiB* mutant and a *invA spiB cyxA* mutant (Figure 3A). Thus, virulence factors were required for cytochrome *bd*-II oxidase-mediated growth at later times after antibiotic treatment.

We next investigated whether the degree of *Clostridia* depletion differed at later time points after infection between mice inoculated with virulent or avirulent *S.* Typhimurium strains. Strikingly, by 4 days after infection of streptomycin-treated mice with avirulent *S.* Typhimurium strains, the abundance of *Clostridia* had recovered to levels similar to those observed in mock-treated mice (Figure 1I), and butyrate levels in the colon were significantly ($p < 0.001$) elevated compared to concentrations measured 1 day after streptomycin treatment (Figure 3D). In stark contrast, a marked depletion of *Clostridia* DNA was still observed 4 days after infection with virulent *S.* Typhimurium strains (Figure 1I), and colonic butyrate concentrations remained at levels observed 1 day after treatment with streptomycin (Figure 3D). While virulence factors reduced butyrate levels by two orders of magnitude (Figure 3D), acetate levels remained unchanged (Figure 3E), and a 5.5-fold change in propionate levels was seen (Figure 3F).

Collectively, these data suggested that virulence factors were unessential for aerobic *S.* Typhimurium growth during early stages of infection when antibiotics maintained a depletion of *Clostridia*. However, once the effect of antibiotics wore off, *Clostridia* levels began to rebound and butyrate concentrations started to rise again. During this recovery from antibiotic treatment, virulence factors contributed to maintaining *Clostridia* depletion and thus became essential for *cyxA*-dependent aerobic pathogen expansion.

Infection with Virulent *S.* Typhimurium Triggers Dysbiosis Characterized by a Depletion of *Clostridia*

Post-antibiotic pathogen expansion is not likely to represent the true physiological role of cytochrome *bd*-II oxidase, since the *cyxAB* operon is conserved among serovars of *S. enterica*, a species that formed long before the advent of antibiotic therapy. While streptomycin-treatment was solely responsible for *cyxA*-dependent growth of *S.* Typhimurium 1 day after infection, a contribution of virulence factors was apparent at 4 days after infection (Figure 3A). We thus reasoned that at later time points after *S.* Typhimurium infection, the physiological role of *cyxA* might be apparent even in the absence of antibiotic treatment. Since genetically susceptible C57BL/6 mice become moribund at 5 days after infection, we switched to a genetically resistant mouse lineage (CBA mice) to test this idea.

To investigate whether *S*. Typhimurium virulence factors could deplete *Clostridia* in the absence of antibiotic treatment, CBA mice were mock infected or infected with either the *S*. Typhimurium wild-type or an *invA spiB* mutant. Measurement of fecal lipocalin 2, an inflammatory marker, suggested that intestinal inflammation peaked between days 10 and 17 after infection and required intact virulence factors (Figure 4A). Transcript levels of *Kc* (encoding the neutrophil chemoattractant CXCL1), *Mip2* (encoding the neutrophil chemoattractant CXCL2), and *Il17a* (encoding the pro-inflammatory cytokine interleukin [IL]-17A) were significantly elevated in the cecal mucosa at days 10 and 17 after infection with the *S*. Typhimurium wild-type compared to mock-infected and *invA spiB* mutant-infected mice (Figures S3A–S3F). Mice infected with the *S.* Typhimurium wild-type shed numbers of the pathogen in their feces approximately three orders of magnitude higher than mice infected with the *invA spiB* mutant (Figure 4B). Importantly, intestinal inflammation induced by the *S*. Typhimurium wild-type was accompanied by a significant ($p < 0.05$) depletion of *Clostridia* (Figure 4C).

To get a more detailed view of how *S*. Typhimurium infection alters the composition of the microbiota in the cecum, its composition was analyzed by 16S rRNA gene sequencing (16S profiling) at 10 and 17 days after infection. Compared to mock-infected mice, both the relative abundance (Figures 4D, S4A, S5, and S6) and the normalized abundance (Figure 4E) of *Clostridia* were significantly reduced in CBA mice at both 10

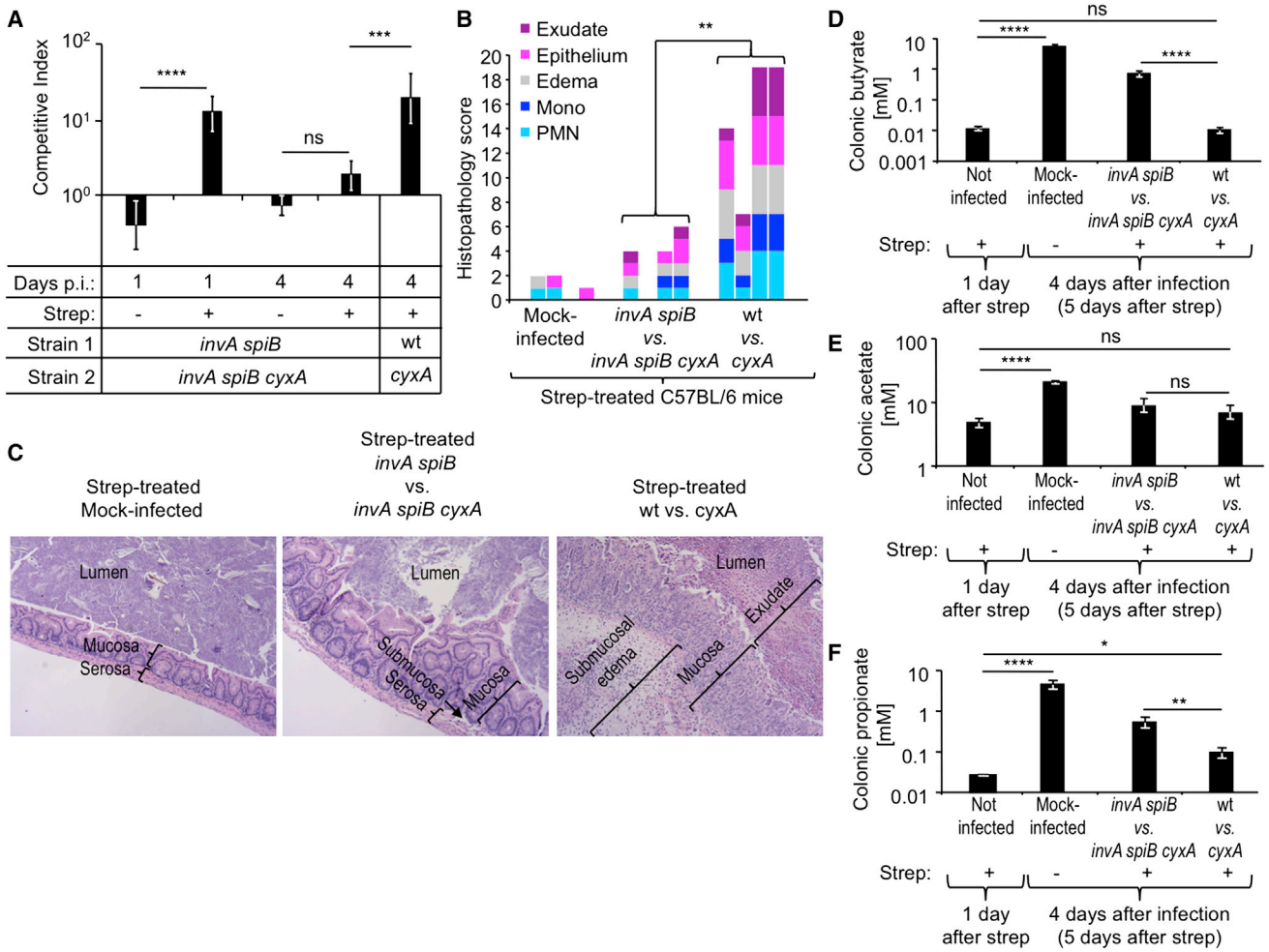

Figure 3. Virulence Factors Drive a Cytochrome *bd*-II Oxidase-Dependent Expansion of *S.* Typhimurium at Later Time Points after Infection

(A–C) Groups of C57BL/6 mice (n is shown in Figure S1A) were mock treated or treated with streptomycin (Strep) and infected 1 day later with the indicated strain mixtures. (A) At 1 and 4 days after infection (Days p.i.), the competitive index (CI) in colon contents was determined. (B) Cecal histopathology was scored using tissue collected 4 days after infection from four mice per group using criteria listed in Table S1 (see also Figure S2). Each bar represents data from one individual animal. (C) Representative images of H&E-stained cecal sections scored in (B). All images were taken at the same magnification.

(D–F) Groups of C57BL/6 mice were treated with streptomycin or mock treated. 1 day after streptomycin treatment organs, were collected for analysis or mice were mock infected or infected with the indicated *S.* Typhimurium strain mixtures. Concentrations of butyrate (D), acetate (E), and propionate (F) in colon contents were determined at the indicated time points.

For (A)–(C) and (D)–(F), bars represent geometric means ± SE. *$p < 0.05$; **$p < 0.01$; ***$p < 0.005$; ****$p < 0.001$; ns, not statistically significantly different; wt, *S.* Typhimurium wild-type.

and 17 days after infection with the *S.* Typhimurium wild-type strain ($p < 0.0001$), but not in *invA spiB* mutant-infected mice. Conversely, the abundance of members from the highly represented phylum *Bacteroidetes* remained unchanged during infection with the *S.* Typhimurium wild-type strain compared to mock-treated mice (Figures 4D, S4B, S5, and S7). Principle coordinate analysis revealed marked changes in the microbial community structure caused by infection with the *S.* Typhimurium wild-type, while the microbiota composition of mice infected with the *invA spiB* mutant was similar to that in mock-infected mice (Figure S3C), which was independent of changes in the abundance of *Enterobacteriaceae* (Figure 4F). The strongest negative correlation in our dataset was that *Clostridia* depletion was accompanied by an expansion of *Gammaproteobacteria* (Figure S3D), the latter of which was due to an increased normalized abundance of *Enterobacteriaceae* (Figure S3E). However, there was no correlation between abundances of *Gammaproteobacteria* and *Bacteroidia* (Figure S3D).

A Luminal Aerobic *S.* Typhimurium Expansion Is Observed in Genetically Resistant Mice in the Absence of Antibiotic Treatment

We next wanted to investigate whether a respiration-dependent expansion could also be observed in the absence of antibiotic treatment. The *cyxA narG napA narZ* genes did not provide a fitness advantage 5 days after competitive infection of CBA mice; however, at days 10 and 17 after infection, the wild-type displayed a significant fitness advantage over the *cyxA narG*

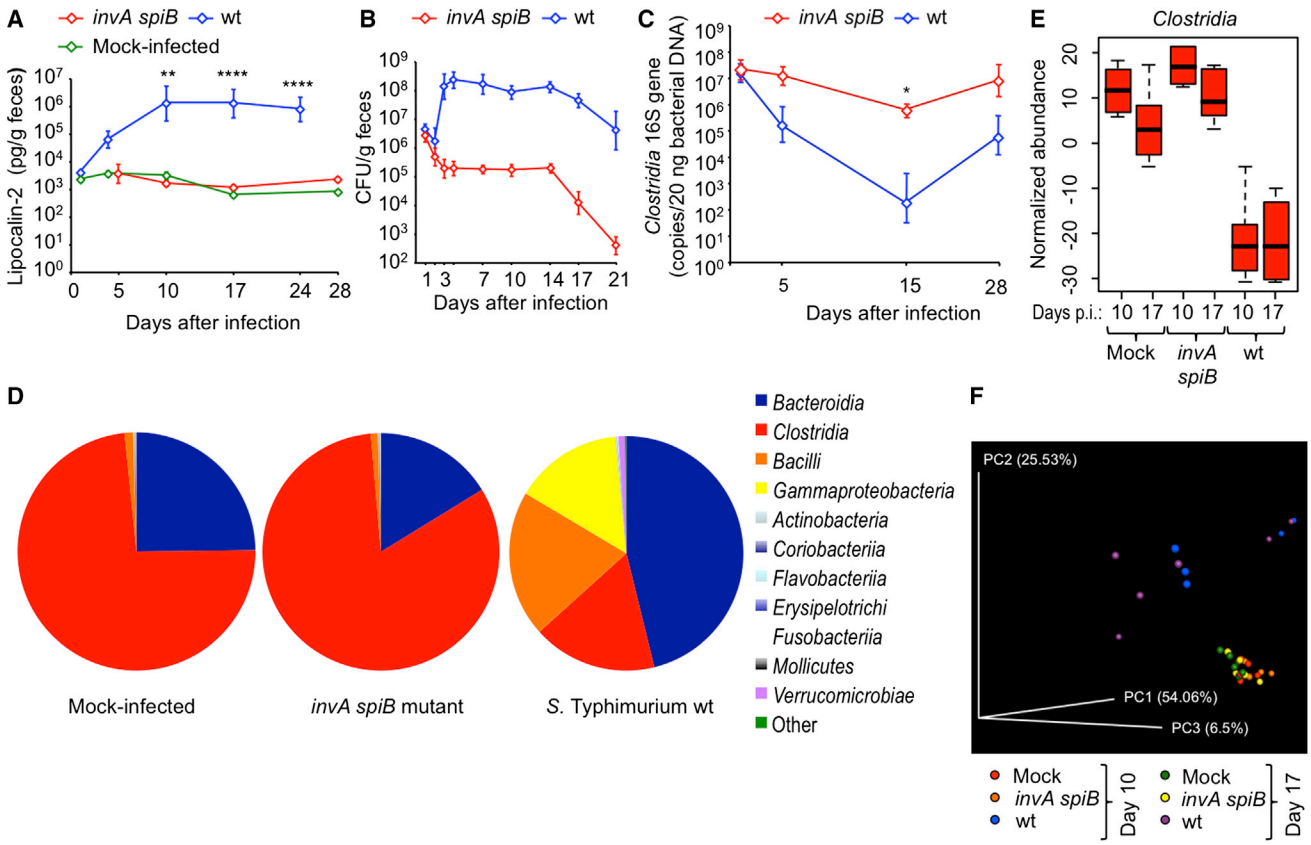

Figure 4. *S.* Typhimurium Virulence Factors Induce Intestinal Inflammation and Are Required for *Clostridia* Depletion in the Absence of Antibiotic Treatment

Groups of CBA mice (n = 6) were mock infected or infected intragastrically with 1 × 10^9 CFU/animal of the virulent *S.* Typhimurium wild-type (wt) or the avirulent *invA spiB* mutant (*invA spiB*).

(A) Fecal lipocalin-2 levels were determined by ELISA (see also Figure S3).

(B) *S.* Typhimurium CFU was determined in the feces over time.

(C) *Clostridia* 16S rRNA gene copy numbers were determined by quantitative real-time PCR.

For (A)–(C), data points represent geometric means ± SE.

(D) Average relative abundances of phylogenetic groupings at the class level determined by 16S profiling of the microbial community present in colon contents on day 10 after infection.

(E) Normalized abundances of members of the class *Clostridia* in colon contents at the indicated days after infection (days p.i.). Boxes in whisker plots represent the second and third quartiles, while lines indicate the first and fourth quartiles.

(F) Weighted principal coordinate analysis of 16S profiling data in which all reads identified as *Enterobacteriaceae* were excluded from analysis. For additional analysis of 16S profiling data, see Figures S4–S7.

Each dot represents data from one animal. *p < 0.05; **p < 0.01; ****p < 0.001.

napA narZ mutant, and by day 28 after infection the *cyxA narG napA narZ* mutant had been cleared from colon contents of most mice (Figure 5A).

Infection of CBA mice with individual *S.* Typhimurium strains revealed that the wild-type was shed in significantly higher numbers in the feces on days 10 and 17 after infection compared to a *cyxA* mutant ($p < 0.05$ and $p < 0.01$, respectively), a *narG napA narZ* mutant ($p < 0.01$ and $p < 0.05$, respectively), or a *cyxA narG napA narZ* mutant ($p < 0.01$ and $p < 0.0001$, respectively) (Figure 5B). At the peak of fecal shedding (day 17 after infection), the *cyxA narG napA narZ* mutant was shed in significantly lower numbers with the feces than either the *cyxA* mutant ($p < 0.05$) or the *narG napA narZ* mutant ($p < 0.05$).

To test the hypothesis that a depletion of *Clostridia* was responsible for a *cyxA*-dependent pathogen expansion, CBA mice were infected intragastrically with a 1:1 mixture of the *S.* Typhimurium wild-type and a *cyxA* mutant. At days 5, 7, and 10 after infection, mice were mock treated or inoculated intragastrically with a community of 17 human *Clostridia* isolates. The *cyxA* gene conferred a significant ($p < 0.005$) fitness advantage at 11 days after infection of mock-treated mice (Figure 6A), which was abrogated in mice inoculated with a community of 17 human *Clostridia* isolates. Furthermore, *S.* Typhimurium infection significantly ($p < 0.001$) diminished cecal butyrate concentrations. While inoculation with a community of 17 human *Clostridia* isolates resulted in a significant ($p < 0.05$) increase in butyrate levels (Figure 6B), cecal levels of acetate and propionate remained unchanged (Figures 6C and 6D). Importantly, colonocytes of mock-infected mice exhibited hypoxia (Figure 6E), which was eliminated during *S.* Typhimurium infection

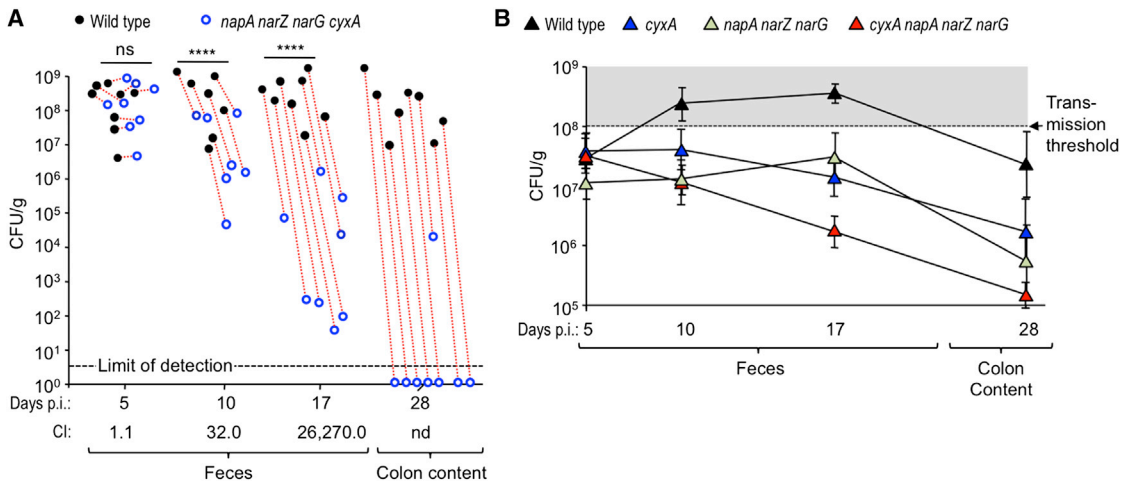

Figure 5. Cytochrome *bd*-II Oxidase and Nitrate Reductases Contribute to a Luminal *S.* Typhimurium Expansion in the Absence of Antibiotic Treatment

(A) Groups of CBA mice were infected intragastrically with a 1:1 mixture of the *S.* Typhimurium wild-type (black circles) and the respiration-deficient *napA narZ narG cyxA* mutant (blue circles), and samples were collected at the indicated days after infection (days p.i.). Dotted red lines connect strains recovered from the same animal. CI, competitive index; ****$p < 0.001$; ns, not statistically significantly different; nd, not determined.

(B) Groups of CBA mice (n = 4) were infected intragastrically with 1×10^8 CFU/animal of one of the indicated *S.* Typhimurium strains, and samples were collected at the indicated days after infection.

(Figure 6F), but could be restored by inoculation with a community of 17 human *Clostridia* isolates (Figure 6G).

Cytochrome *bd*-II Oxidase and Nitrate Reductases Are Required for Transmission by the Fecal-Oral Route

Maximal bacterial shedding is relevant because *S.* Typhimurium numbers in the feces need to exceed a threshold of 10^8 bacteria per gram feces for transmission (Lawley et al., 2008). Interestingly, only the *S.* Typhimurium wild-type always exceeded this critical threshold during infection of CBA mice (Figure 5B). To test the prediction that respiration is required for transmission, we studied transmission of *S.* Typhimurium from infected CBA mice to naive CBA mice. All naive mice cohoused with *S.* Typhimurium wild-type-infected mice started to shed the pathogen within 7 days of cohousing (Figure 7). In contrast, the pathogen could not be isolated from any of the naive mice cohoused with either *cyxA* mutant-infected mice or with *cyxA narG napA narZ* mutant-infected mice after 7 days of cohousing. After 18 days of cohousing, 33% of naive mice cohoused with *cyxA* mutant-infected mice became colonized with the pathogen. However, none of the naive mice cohoused for 18 days with *cyxA narG napA narZ* mutant-infected mice became colonized with the pathogen. Thus, aerobic respiration contributed to transmission, but an inability to respire both oxygen and nitrate resulted in complete loss of *S.* Typhimurium transmissibility by the fecal-oral route.

DISCUSSION

The intestine is home to a large microbial community that confers benefit by preventing pathogen expansion (Bohnhoff et al., 1954). Streptomycin treatment of mice depletes populations of spore-forming bacteria belonging to the class *Clostridia* (Sekirov et al., 2008), which are the members within the community that are most effective in preventing expansion of commensal *E. coli* in the mouse intestine (Itoh and Freter, 1989). *Clostridia* become depleted at later stages of an *S.* Typhimurium infection in streptomycin-treated mice through a neutrophil-dependent mechanism (Gill et al., 2012). Here, we show that inflammation induced by *S.* Typhimurium virulence factors leads to a depletion of *Clostridia* in genetically resistant mice even in the absence of antibiotic treatment.

Changes in the microbiota composition induced either by streptomycin treatment or by *S.* Typhimurium infection were accompanied by a depletion of the short-chain fatty acid butyrate. Butyrate production by the gut microbiota proceeds through the acetyl-CoA pathway, the glutarate pathway, the 4-aminobutyrate pathway, or the lysine pathway, and the majority of bacteria encoding these pathways are members of the class *Clostridia* (Louis and Flint, 2009; Vital et al., 2014). An antibiotic-induced depletion of short-chain fatty acids has been previously implicated in the loss of colonization resistance against *S.* Typhimurium (Garner et al., 2009; Meynell, 1963). However, the mechanism by which short-chain fatty acids limit pathogen expansion is not fully resolved. Butyrate has a marked influence on host cell physiology because it serves as the main energy source for colonocytes (Donohoe et al., 2012). The main function of the colon is to absorb water by generating an osmotic gradient through the absorption of sodium (Na^+). Na^+ diffuses along an electrochemical gradient through channels located in the apical membrane of surface colonocytes and is then actively extruded by a Na^+ pump (Na^+ K^+ ATPase) located in their basolateral membrane (Sandle, 1998). The ATP required by surface colonocytes to energize Na^+ transport comes from the oxidation of microbiota-derived butyrate to carbon dioxide (CO_2) (Velázquez et al., 1997). The oxidation of butyrate to CO_2 consumes considerable quantities of oxygen within the host cell, thereby rendering the epithelium hypoxic (<7.6 mmHg or <1% O_2)

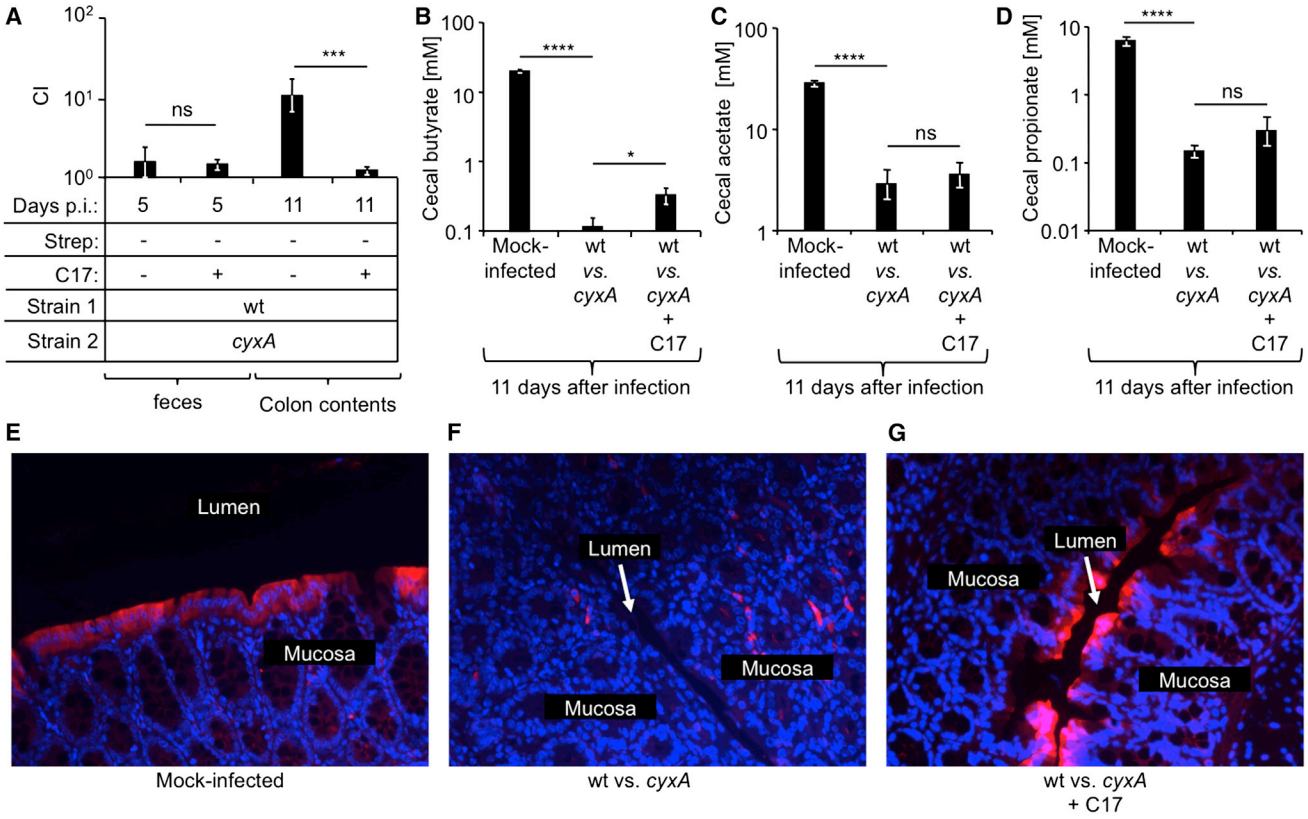

Figure 6. Depletion of *Clostridia* Increases Colonocyte Oxygenation and Drives a Cytochrome *bd*-II Oxidase-Dependent Expansion of *S.* Typhimurium

Groups of CBA mice were mock infected or infected intragastrically with a 1:1 mixture of the *S.* Typhimurium wild-type (wt) and a *cyxA* mutant. At 5, 7, and 10 days after infection, mice were mock inoculated or inoculated with 17 human *Clostridia* isolates (C17).

(A) The competitive index (CI) in feces or colon contents was determined at the indicated time points.

(B–D) Concentrations of butyrate (B), acetate (C), and propionate (D) in cecal contents are shown.

For (A)–(D), bars represent geometric means ± SE.

(E–G) Binding of pimonidazole (red fluorescence) was detected in colonic sections counter-stained with DAPI nuclear stain (blue fluorescence). Representative images are shown. *p < 0.05; ***p < 0.005; ****p < 0.001; ns, not statistically significantly different.

(reviewed in Colgan and Taylor, 2010). Importantly, a streptomycin-mediated depletion of *Clostridia*-derived butyrate changes the energy metabolism of colonocytes toward fermentation of glucose, thereby conserving oxygen within the host cell and increasing oxygenation of the epithelium (Kelly et al., 2015). Since oxygen diffuses freely across biological membranes, increased oxygenation of the epithelium is predicted to elevate oxygen availability in the intestinal lumen (Espey, 2013). Consistent with this idea, we found that streptomycin treatment fueled a *cyxA*-dependent aerobic expansion of *S.* Typhimurium, which could be blunted by increasing the abundance of *Clostridia* or by restoring the physiologic hypoxia of colonocytes through tributyrin supplementation.

Streptomycin treatment depleted *Clostridia* within a day, while *S.* Typhimurium infection alone reduced the prevalence of *Clostridia* within the community more slowly. It has been reported previously that streptomycin treatment can rescue the ability of an *S.* Typhimurium mutant lacking both T3SS-1 and T3SS-2 to colonize the lumen of the large bowel at early stages of infection (Barthel et al., 2003). Our data indicate that this effect is at least in part due to increased oxygenation of the intestinal epithelium driving a *cyxA*-dependent aerobic expansion of *S.* Typhimurium. Interestingly, our data suggest that virulence factors and antibiotic treatment drive pathogen expansion through the same mechanism, namely a depletion of *Clostridia*. The biological significance of this pathogen expansion is that shedding of the pathogen in high numbers with the feces is required for its successful transmission by the fecal-oral route (Lawley et al., 2008). Consistent with this idea, we found that a respiration-dependent expansion of *S.* Typhimurium was essential for transmission of the pathogen in the mouse model.

The picture emerging from this study is that *S.* Typhimurium uses its virulence factors to deplete butyrate-producing *Clostridia* from the gut-associated microbial community. The resulting increase in epithelial oxygenation drives a cytochrome *bd*-II oxidase-dependent aerobic expansion of *S.* Typhimurium within the gut lumen, which synergizes with a nitrate respiration-driven expansion to enhance transmission. This pathogenic strategy is exacerbated by oral antibiotic therapy since it enhances and accelerates *Clostridia* depletion, which might explain why treatment with oral antibiotics often precedes infection

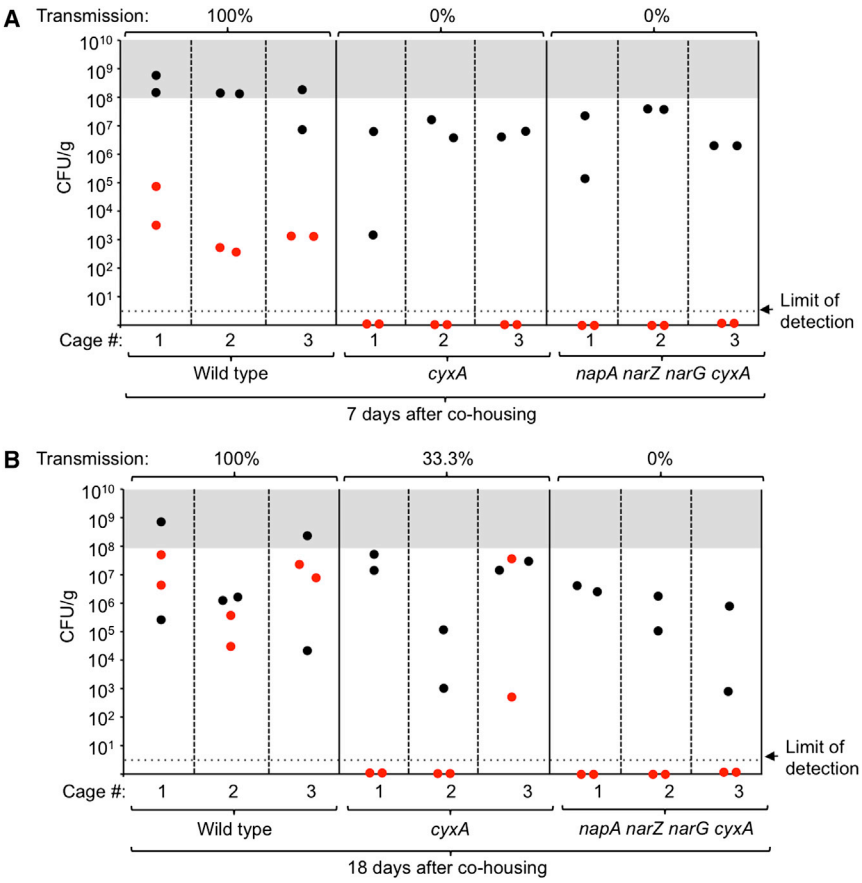

Figure 7. Respiration Is Required for Fecal-Oral Transmission

(A and B) Groups of CBA mice (n = 6) were infected intragastrically with 1 × 10^8 CFU/animal of either the *S.* Typhimurium wild-type, a *cyxA* mutant, or a *napA narZ narG cyxA* mutant. 10 days after infection, two infected mice (donors, black circles) were co-housed with two naive mice (recipients, red circles) per cage, and feces (A) or colon contents (B) were collected after 7 (A) or 18 (B) days of co-housing.

with antibiotic-sensitive *S. enterica* serovars causing human gastroenteritis (Pavia et al., 1990).

EXPERIMENTAL PROCEDURES

Bacterial Strains and Plasmids

The 17 human *Clostridia* isolates were kindly provided by K. Honda (Atarashi et al., 2011; Narushima et al., 2014) and were cultured individually as described previously (Atarashi et al., 2013). *S.* Typhimurium and *E. coli* strains used in this study are listed in Table S1, and culture conditions are described in the Supplemental Experimental Procedures. The plasmids and primers used in this study are listed in Tables S2 and S3, respectively. Construction of *S.* Typhimurium mutants and plasmids is described in the Supplemental Experimental Procedures.

Animal Experiments

All experiments in this study were approved by the Institutional Animal Care and Use Committee at the University of California at Davis.

Female C57BL/6 mice, aged 8–12 weeks, and female CBA mice, aged 6–8 weeks, were obtained from The Jackson Laboratory (C57BL/6J mice; CBA/J mice). C57BL/6 mice were treated with 20 mg/animal streptomycin or mock treated and orally inoculated 24 hr later with *S.* Typhimurium strains as described in the Supplemental Experimental Procedures. For tributyrin supplementation, mice were mock treated or received tributyrin (5 g/kg) by oral gavage 3 hr after infection. CBA mice were inoculated with *S.* Typhimurium strains as described in the Supplemental Experimental Procedures. For microbiota analysis, mice were euthanized at 10 and 17 days after infection, and DNA from the cecal contents was extracted using the PowerSoil DNA Isolation kit (Mo-Bio) according to the manufacturer's protocol. Generation and analysis of sequencing data are described in detail in the Supplemental Experimental Procedures. Transmission was studied as described previously (Lawley et al., 2008) and is described in detail in the Supplemental Experimental Procedures. Inoculation of mice with a community of 17 *Clostridia* strains or with spore preparations is described in the Supplemental Experimental Procedures. In some experiments Pimonidazole hydrochloride (PMDZ) (Hypoxyprobe) was administered by intraperitoneal injection at a dosage of approximately 60 mg/kg body weight 60 min prior to euthanasia.

Analysis of Animal Samples

Hypoxia staining was performed as described previously (Kelly et al., 2015) and is described in detail in the Supplemental Experimental Procedures. Blinded evaluation of histopathological changes was performed as described previously (Spees et al., 2013) using the criteria listed in Table S4. Short-chain fatty acid concentrations in cecal and colon contents were determined by mass spectrometer as described in the Supplemental Experimental Procedures. RNA was isolated from tissue using standard methods (see Supplemental Experimental Procedures for details) and reverse transcribed using random hexamers and Moloney murine leukemia virus reverse transcriptase (Applied Biosystems). Quantitative real-time PCR was performed using SYBR green (Applied Biosystems) PCR mix and the appropriate primer sets (Table S2) at a final concentration of 0.25 mM. Absolute values were calculated using a plasmid carrying the cloned gene to generate a standard curve using concentrations ranging from 10^8 to 10^1 copies/μl diluted in a 0.02 mg/ml yeast RNA (Sigma) solution.

Statistical Analysis

Fold changes of ratios (bacterial numbers or mRNA levels) were transformed logarithmically prior to statistical analysis. An unpaired Student's t test was used to determine whether differences in fold changes between groups were statistically significant ($p < 0.05$). Significance of differences in histopathology scores was determined by a one-tailed non-parametric test (Mann-Whitney).

ACCESSION NUMBERS

The accession numbers for the data reported in this paper are NCBI BioSample: SAMN04543794, SAMN04543795, SAMN04543796, SAMN04543797, SAMN04543798, SAMN04543799, SAMN04543800, SAMN04543801, SAMN04543802, SAMN04543803, SAMN04543804, SAMN04543805, SAMN04543806, SAMN04543807, SAMN04543808, SAMN04543809, SAMN04543810, SAMN04543811, SAMN04543812, SAMN04543813, SAMN04543814, SAMN04543815, SAMN04543816, SAMN04543817, SAMN04543818, SAMN04543819, SAMN04543820, SAMN04543821, SAMN04543822, SAMN04543823, SAMN04543824, SAMN04543825, SAMN04543826, SAMN04543827, SAMN04543828.

SUPPLEMENTAL INFORMATION

Supplemental Information includes Supplemental Experimental Procedures, seven figures, and four tables and can be found with this article online at http://dx.doi.org/10.1016/j.chom.2016.03.004.

AUTHOR CONTRIBUTIONS

F.R.-C., L.F.Z., F.F., C.A.L., M.X.B., and E.E.O. performed and analyzed the experiments. G.X., C.B.L., and S.E.W. performed experiments. F.R.-C. and A.J.B. were responsible for the overall study design and for writing the manuscript.

ACKNOWLEDGMENTS

We would like to acknowledge K. Honda for kindly providing 17 human *Clostridia* isolates and the Host-Microbe Systems Biology Core at UC for expert technical assistance with microbiota sequence analysis. This work was supported by Public Health Service Grants AI096528 (A.J.B.), AI112949 (A.J.B.), AI103248 (S.E.W.), AI112241 (C.A.L.), OD010931 (E.M.V.), and AI060555 (E.M.V. and F.R.-C.).

Received: November 23, 2015
Revised: February 17, 2016
Accepted: March 17, 2016
Published: April 13, 2016

REFERENCES

Alexeeva, S., Hellingwerf, K.J., and Teixeira de Mattos, M.J. (2003). Requirement of ArcA for redox regulation in Escherichia coli under microaerobic but not anaerobic or aerobic conditions. J. Bacteriol. *185*, 204–209.

Ali, M.M., Newsom, D.L., González, J.F., Sabag-Daigle, A., Stahl, C., Steidley, B., Dubena, J., Dyszel, J.L., Smith, J.N., Dieye, Y., et al. (2014). Fructose-asparagine is a primary nutrient during growth of Salmonella in the inflamed intestine. PLoS Pathog. *10*, e1004209.

Aserkoff, B., and Bennett, J.V. (1969). Effect of antibiotic therapy in acute salmonellosis on the fecal excretion of salmonellae. N. Engl. J. Med. *281*, 636–640.

Atarashi, K., Tanoue, T., Shima, T., Imaoka, A., Kuwahara, T., Momose, Y., Cheng, G., Yamasaki, S., Saito, T., Ohba, Y., et al. (2011). Induction of colonic regulatory T cells by indigenous Clostridium species. Science *331*, 337–341.

Atarashi, K., Tanoue, T., Oshima, K., Suda, W., Nagano, Y., Nishikawa, H., Fukuda, S., Saito, T., Narushima, S., Hase, K., et al. (2013). Treg induction by a rationally selected mixture of Clostridia strains from the human microbiota. Nature *500*, 232–236.

Atlung, T., and Brøndsted, L. (1994). Role of the transcriptional activator AppY in regulation of the cyx appA operon of Escherichia coli by anaerobiosis, phosphate starvation, and growth phase. J. Bacteriol. *176*, 5414–5422.

Barman, M., Unold, D., Shifley, K., Amir, E., Hung, K., Bos, N., and Salzman, N. (2008). Enteric salmonellosis disrupts the microbial ecology of the murine gastrointestinal tract. Infect. Immun. *76*, 907–915.

Barthel, M., Hapfelmeier, S., Quintanilla-Martínez, L., Kremer, M., Rohde, M., Hogardt, M., Pfeffer, K., Rüssmann, H., and Hardt, W.D. (2003). Pretreatment of mice with streptomycin provides a Salmonella enterica serovar Typhimurium colitis model that allows analysis of both pathogen and host. Infect. Immun. *71*, 2839–2858.

Bohnhoff, M., Drake, B.L., and Miller, C.P. (1954). Effect of streptomycin on susceptibility of intestinal tract to experimental Salmonella infection. Proc. Soc. Exp. Biol. Med. *86*, 132–137.

Brøndsted, L., and Atlung, T. (1996). Effect of growth conditions on expression of the acid phosphatase (cyx-appA) operon and the appY gene, which encodes a transcriptional activator of Escherichia coli. J. Bacteriol. *178*, 1556–1564.

Carreau, A., El Hafny-Rahbi, B., Matejuk, A., Grillon, C., and Kieda, C. (2011). Why is the partial oxygen pressure of human tissues a crucial parameter? Small molecules and hypoxia. J. Cell. Mol. Med. *15*, 1239–1253.

Colgan, S.P., and Taylor, C.T. (2010). Hypoxia: an alarm signal during intestinal inflammation. Nat. Rev. Gastroenterol. Hepatol. *7*, 281–287.

Cotter, P.A., and Gunsalus, R.P. (1992). Contribution of the fnr and arcA gene products in coordinate regulation of cytochrome o and d oxidase (cyoABCDE and cydAB) genes in Escherichia coli. FEMS Microbiol. Lett. *70*, 31–36.

Cotter, P.A., Chepuri, V., Gennis, R.B., and Gunsalus, R.P. (1990). Cytochrome o (cyoABCDE) and d (cydAB) oxidase gene expression in Escherichia coli is regulated by oxygen, pH, and the fnr gene product. J. Bacteriol. *172*, 6333–6338.

Cotter, P.A., Darie, S., and Gunsalus, R.P. (1992). The effect of iron limitation on expression of the aerobic and anaerobic electron transport pathway genes in Escherichia coli. FEMS Microbiol. Lett. *100*, 227–232.

Craig, M., Sadik, A.Y., Golubeva, Y.A., Tidhar, A., and Slauch, J.M. (2013). Twin-arginine translocation system (tat) mutants of Salmonella are attenuated due to envelope defects, not respiratory defects. Mol. Microbiol. *89*, 887–902.

Dassa, J., Fsihi, H., Marck, C., Dion, M., Kieffer-Bontemps, M., and Boquet, P.L. (1991). A new oxygen-regulated operon in Escherichia coli comprises the genes for a putative third cytochrome oxidase and for pH 2.5 acid phosphatase (appA). Mol. Gen. Genet. *229*, 341–352.

Donohoe, D.R., Wali, A., Brylawski, B.P., and Bultman, S.J. (2012). Microbial regulation of glucose metabolism and cell-cycle progression in mammalian colonocytes. PLoS ONE *7*, e46589.

Espey, M.G. (2013). Role of oxygen gradients in shaping redox relationships between the human intestine and its microbiota. Free Radic. Biol. Med. *55*, 130–140.

Fu, H.A., Iuchi, S., and Lin, E.C. (1991). The requirement of ArcA and Fnr for peak expression of the cyd operon in Escherichia coli under microaerobic conditions. Mol. Gen. Genet. *226*, 209–213.

Galán, J.E., and Curtiss, R., 3rd (1989). Cloning and molecular characterization of genes whose products allow Salmonella typhimurium to penetrate tissue culture cells. Proc. Natl. Acad. Sci. USA *86*, 6383–6387.

Garner, C.D., Antonopoulos, D.A., Wagner, B., Duhamel, G.E., Keresztes, I., Ross, D.A., Young, V.B., and Altier, C. (2009). Perturbation of the small intestine microbial ecology by streptomycin alters pathology in a Salmonella enterica serovar typhimurium murine model of infection. Infect. Immun. *77*, 2691–2702.

Gill, N., Ferreira, R.B., Antunes, L.C., Willing, B.P., Sekirov, I., Al-Zahrani, F., Hartmann, M., and Finlay, B.B. (2012). Neutrophil elastase alters the murine gut microbiota resulting in enhanced Salmonella colonization. PLoS ONE *7*, e49646.

Hensel, M., Shea, J.E., Gleeson, C., Jones, M.D., Dalton, E., and Holden, D.W. (1995). Simultaneous identification of bacterial virulence genes by negative selection. Science *269*, 400–403.

Itoh, K., and Freter, R. (1989). Control of Escherichia coli populations by a combination of indigenous clostridia and lactobacilli in gnotobiotic mice and continuous-flow cultures. Infect. Immun. *57*, 559–565.

Kelly, C.J., Zheng, L., Campbell, E.L., Saeedi, B., Scholz, C.C., Bayless, A.J., Wilson, K.E., Glover, L.E., Kominsky, D.J., Magnuson, A., et al. (2015). Crosstalk between Microbiota-Derived Short-Chain Fatty Acids and Intestinal Epithelial HIF Augments Tissue Barrier Function. Cell Host Microbe *17*, 662–671.

Kizaka-Kondoh, S., and Konse-Nagasawa, H. (2009). Significance of nitroimidazole compounds and hypoxia-inducible factor-1 for imaging tumor hypoxia. Cancer Sci. *100*, 1366–1373.

Lawley, T.D., Bouley, D.M., Hoy, Y.E., Gerke, C., Relman, D.A., and Monack, D.M. (2008). Host transmission of Salmonella enterica serovar Typhimurium is controlled by virulence factors and indigenous intestinal microbiota. Infect. Immun. *76*, 403–416.

Lopez, C.A., Winter, S.E., Rivera-Chávez, F., Xavier, M.N., Poon, V., Nuccio, S.P., Tsolis, R.M., and Bäumler, A.J. (2012). Phage-mediated acquisition of a type III secreted effector protein boosts growth of salmonella by nitrate respiration. MBio *3*, 3.

Lopez, C.A., Rivera-Chávez, F., Byndloss, M.X., and Bäumler, A.J. (2015). The periplasmic nitrate reductase NapABC supports luminal growth of Salmonella enterica serovar Typhimurium during colitis. Infect. Immun. *83*, 3470–3478.

Louis, P., and Flint, H.J. (2009). Diversity, metabolism and microbial ecology of butyrate-producing bacteria from the human large intestine. FEMS Microbiol. Lett. *294*, 1–8.

Majowicz, S.E., Musto, J., Scallan, E., Angulo, F.J., Kirk, M., O'Brien, S.J., Jones, T.F., Fazil, A., and Hoekstra, R.M.; International Collaboration on Enteric Disease 'Burden of Illness' Studies (2010). The global burden of nontyphoidal Salmonella gastroenteritis. Clin. Infect. Dis. *50*, 882–889.

McClelland, M., Sanderson, K.E., Spieth, J., Clifton, S.W., Latreille, P., Courtney, L., Porwollik, S., Ali, J., Dante, M., Du, F., et al. (2001). Complete genome sequence of Salmonella enterica serovar Typhimurium LT2. Nature *413*, 852–856.

Meynell, G.G. (1963). Antibacterial mechanisms of the mouse gut. II. The role of Eh and volatile fatty acids in the normal gut. Br. J. Exp. Pathol. *44*, 209–219.

Narushima, S., Sugiura, Y., Oshima, K., Atarashi, K., Hattori, M., Suematsu, M., and Honda, K. (2014). Characterization of the 17 strains of regulatory T cell-inducing human-derived Clostridia. Gut Microbes *5*, 333–339.

Nelson, J.D., Kusmiesz, H., Jackson, L.H., and Woodman, E. (1980). Treatment of Salmonella gastroenteritis with ampicillin, amoxicillin, or placebo. Pediatrics *65*, 1125–1130.

Pavia, A.T., Shipman, L.D., Wells, J.G., Puhr, N.D., Smith, J.D., McKinley, T.W., and Tauxe, R.V. (1990). Epidemiologic evidence that prior antimicrobial exposure decreases resistance to infection by antimicrobial-sensitive Salmonella. J. Infect. Dis. *161*, 255–260.

Que, J.U., and Hentges, D.J. (1985). Effect of streptomycin administration on colonization resistance to Salmonella typhimurium in mice. Infect. Immun. *48*, 169–174.

Rivera-Chávez, F., Winter, S.E., Lopez, C.A., Xavier, M.N., Winter, M.G., Nuccio, S.P., Russell, J.M., Laughlin, R.C., Lawhon, S.D., Sterzenbach, T., et al. (2013). Salmonella uses energy taxis to benefit from intestinal inflammation. PLoS Pathog. *9*, e1003267.

Sandle, G.I. (1998). Salt and water absorption in the human colon: a modern appraisal. Gut *43*, 294–299.

Sekirov, I., Tam, N.M., Jogova, M., Robertson, M.L., Li, Y., Lupp, C., and Finlay, B.B. (2008). Antibiotic-induced perturbations of the intestinal microbiota alter host susceptibility to enteric infection. Infect. Immun. *76*, 4726–4736.

Spees, A.M., Wangdi, T., Lopez, C.A., Kingsbury, D.D., Xavier, M.N., Winter, S.E., Tsolis, R.M., and Bäumler, A.J. (2013). Streptomycin-induced inflammation enhances Escherichia coli gut colonization through nitrate respiration. MBio *4*, e00430–e00413.

Stecher, B., Robbiani, R., Walker, A.W., Westendorf, A.M., Barthel, M., Kremer, M., Chaffron, S., Macpherson, A.J., Buer, J., Parkhill, J., et al. (2007). Salmonella enterica serovar typhimurium exploits inflammation to compete with the intestinal microbiota. PLoS Biol. *5*, 2177–2189.

Thiennimitr, P., Winter, S.E., Winter, M.G., Xavier, M.N., Tolstikov, V., Huseby, D.L., Sterzenbach, T., Tsolis, R.M., Roth, J.R., and Bäumler, A.J. (2011). Intestinal inflammation allows Salmonella to use ethanolamine to compete with the microbiota. Proc. Natl. Acad. Sci. USA *108*, 17480–17485.

Tseng, C.P., Albrecht, J., and Gunsalus, R.P. (1996). Effect of microaerophilic cell growth conditions on expression of the aerobic (cyoABCDE and cydAB) and anaerobic (narGHJI, frdABCD, and dmsABC) respiratory pathway genes in Escherichia coli. J. Bacteriol. *178*, 1094–1098.

Tsolis, R.M., Adams, L.G., Ficht, T.A., and Bäumler, A.J. (1999). Contribution of Salmonella typhimurium virulence factors to diarrheal disease in calves. Infect. Immun. *67*, 4879–4885.

Velázquez, O.C., Lederer, H.M., and Rombeau, J.L. (1997). Butyrate and the colonocyte. Production, absorption, metabolism, and therapeutic implications. Adv. Exp. Med. Biol. *427*, 123–134.

Vital, M., Howe, A.C., and Tiedje, J.M. (2014). Revealing the bacterial butyrate synthesis pathways by analyzing (meta)genomic data. MBio *5*, e00889.

Winter, S.E., Thiennimitr, P., Winter, M.G., Butler, B.P., Huseby, D.L., Crawford, R.W., Russell, J.M., Bevins, C.L., Adams, L.G., Tsolis, R.M., et al. (2010). Gut inflammation provides a respiratory electron acceptor for Salmonella. Nature *467*, 426–429.

Cell Host & Microbe, Volume *19*

Supplemental Information

Depletion of Butyrate-Producing *Clostridia* from the Gut Microbiota Drives an Aerobic Luminal Expansion of *Salmonella*

Fabian Rivera-Chávez, Lillian F. Zhang, Franziska Faber, Christopher A. Lopez, Mariana X. Byndloss, Erin E. Olsan, Gege Xu, Eric M. Velazquez, Carlito B. Lebrilla, Sebastian E. Winter, and Andreas J. Bäumler

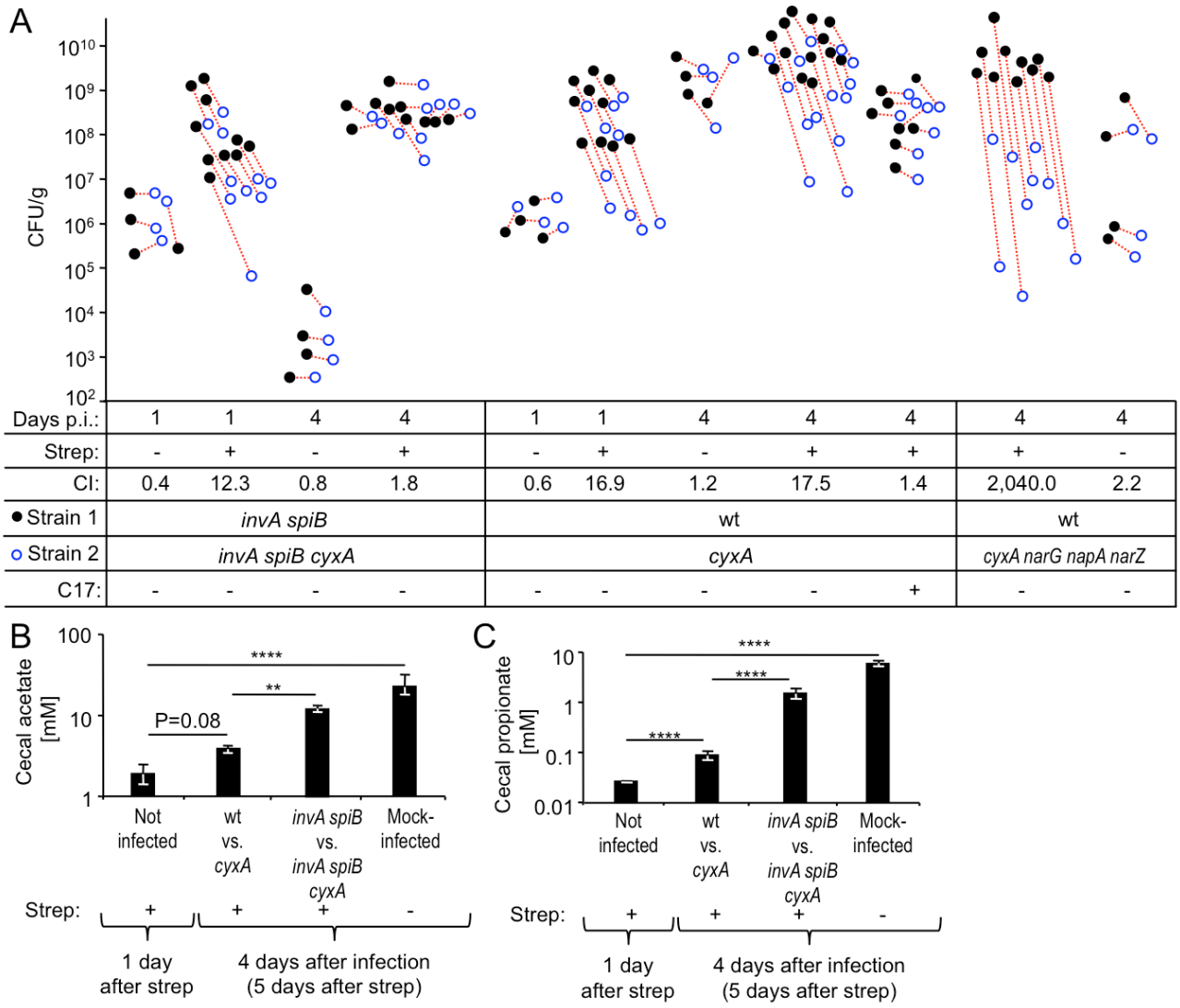

Days p.i.:	1	1	4	4	1	1	4	4	4	4	4
Strep:	-	+	-	+	-	+	-	+	+	+	-
CI:	0.4	12.3	0.8	1.8	0.6	16.9	1.2	17.5	1.4	2,040.0	2.2
● Strain 1	*invA spiB*				wt					wt	
○ Strain 2	*invA spiB cyxA*				*cyxA*					*cyxA narG napA narZ*	
C17:	-	-	-	-	-	-	-	-	+	-	-

Figure S1: Streptomycin treatment depletes short-chain fatty acids and drives an aerobic luminal expansion of *Salmonella* (related to Figures 1 - 3).

(A) Colony-forming units (CFU) recovered from individual mice in experiments shown in figure panels 1D, 1E, and 3A. Groups of C57BL/6 mice were mock-treated or treated with streptomycin (Strep) and one day later infected intragastrically with a 1:1 mixture of the indicated *S.* Typhimurium strains. One day after infection, some mice were inoculated intragastrically with a culture of 17 human *Clostridia* isolates (C17). Samples were collected at the indicated days after infection (days p.i.). Dotted red lines connect strains recovered from the same animal. (B and C) Groups of C57BL/6 mice were treated with streptomycin (Strep) or mock-treated (-) and one day later were mock-infected or infected intragastrically with the indicated *S.* Typhimurium strain mixtures (*n* is indicated in Fig. 1H). The concentration of acetate (B) and propionate (C) was measured in cecal contents at the indicated time points after streptomycin treatment. Bars represent geometric means ± standard error. **, $P < 0.01$; ****, $P < 0.001$; wt, *S.* Typhimurium wild type.

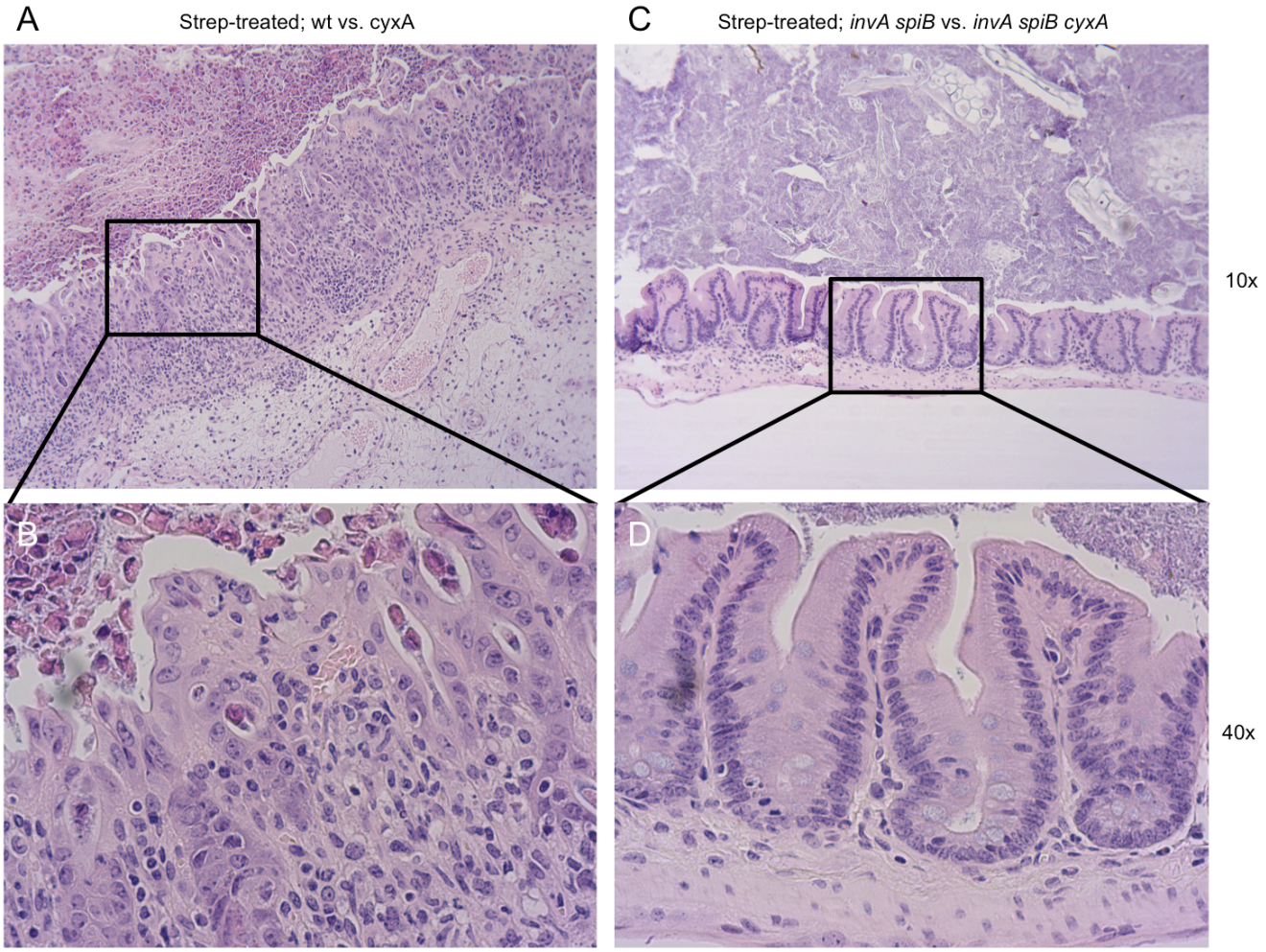

Figure S2: Virulence factors drive pathological changes during *S.* Typhimurium infection (related to Figure 3B).

Groups of C57BL/6 mice (*n* is shown in Fig. S1A) were treated with streptomycin (Strep), infected one day later with the indicated strain mixtures and tissue collected four days after infection. (A-D) Representative images of H/E-stained cecal sections scored in Fig. 3B were taken with a 10x (A and C) or 40x (B and D) objective.

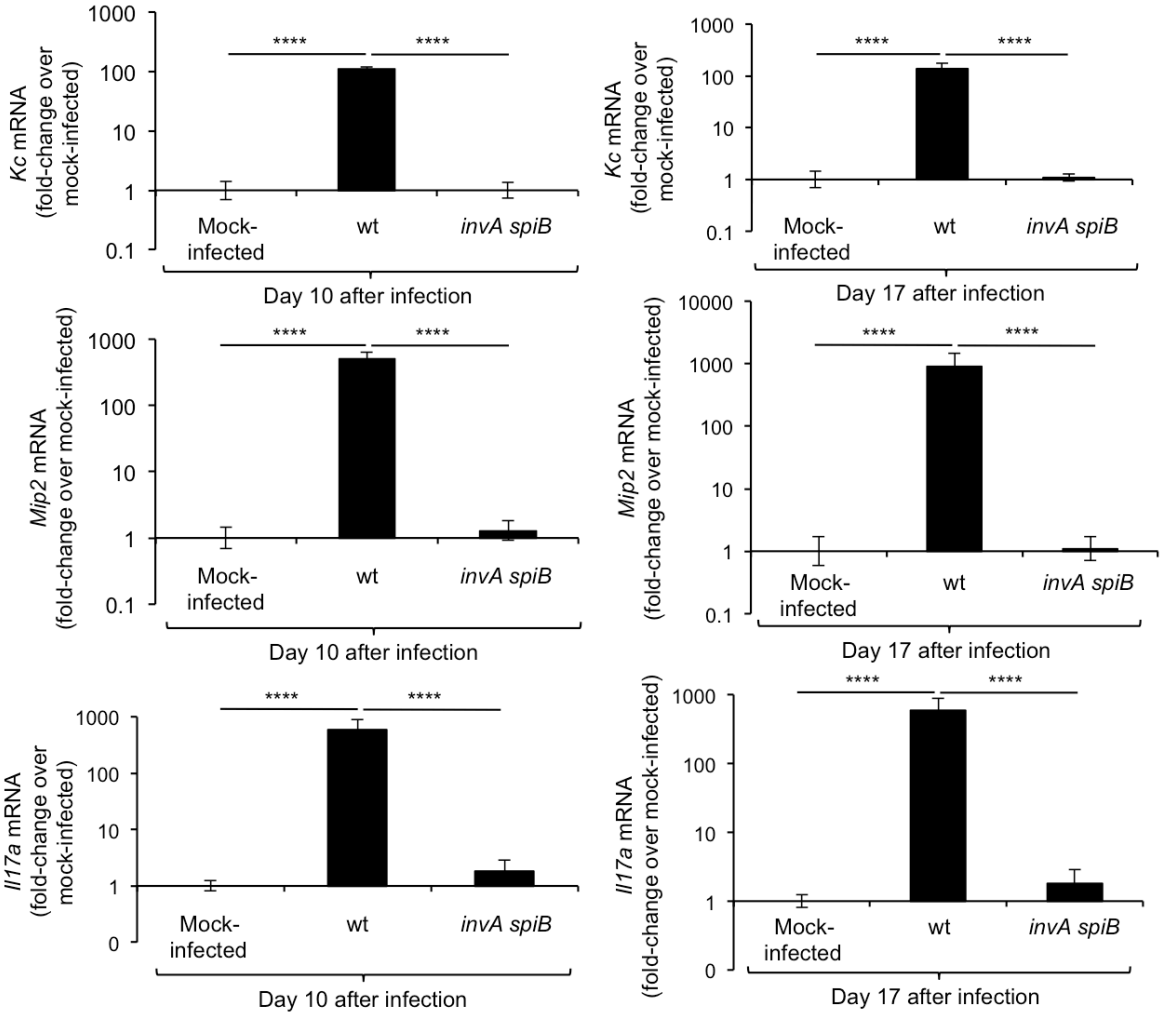

Figure S3: *S.* Typhimurium virulence factors induce elevated transcript levels of pro-inflammatory genes in the cecal mucosa (related to Figure 4A).

Groups of CBA mice (n = 6) were mock-infected or infected intragastrically with 1 x 10^9 CFU/animal of the virulent *S.* Typhimurium wild type (wt) or the avirulent *invA spiB* mutant (*invA spiB*) and the cecum was collected at the indicated time points to isolate RNA. Transcript levels of the indicated genes were determined by quantitative real-time PCR. Data represent geometric means ± standard error of fold-changes over transcript levels detected in mock-infected animals. ****, $P < 0.001$.

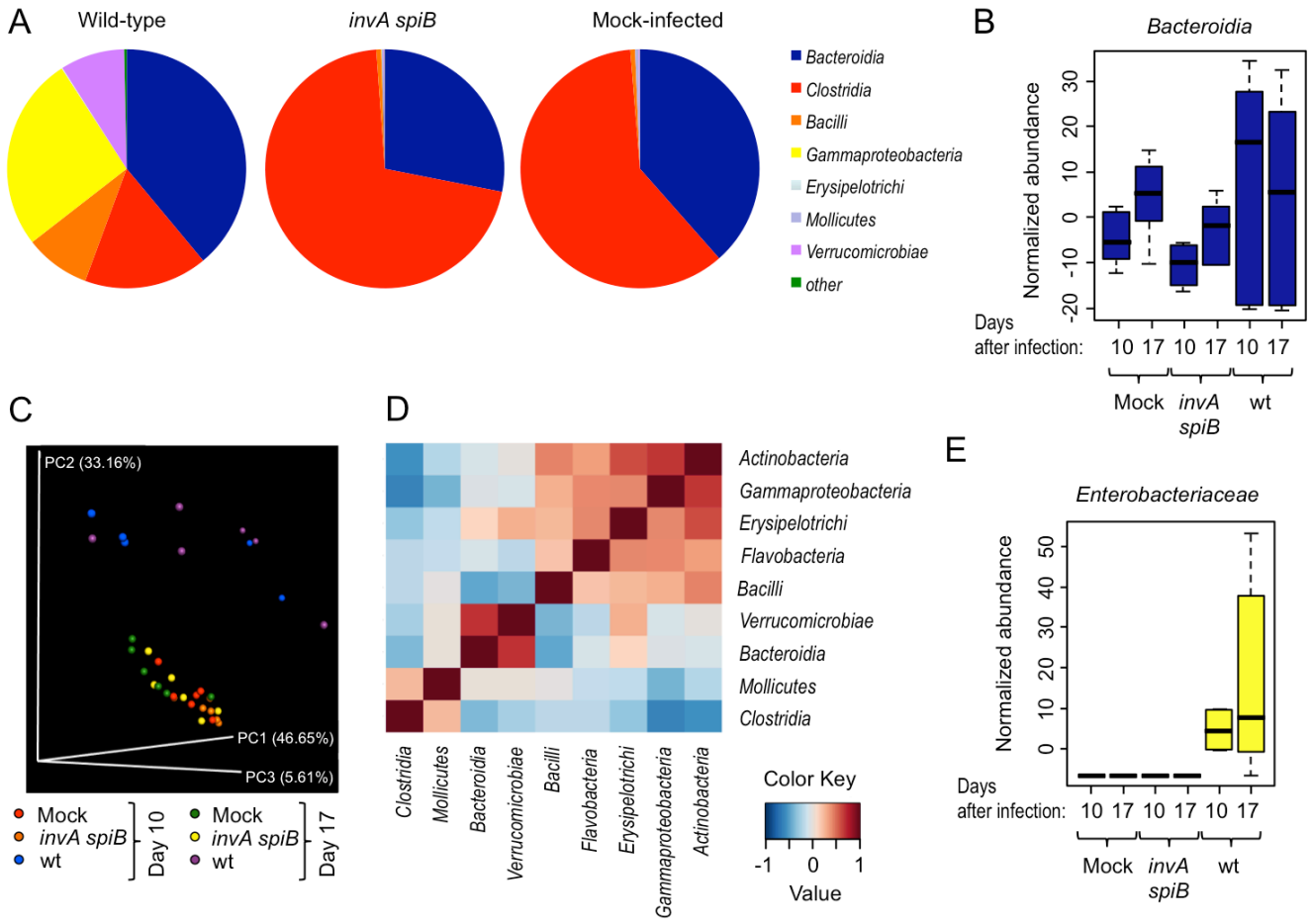

Figure S4: *S.* Typhimurium virulence factors are required for *Clostridia* depletion in the absence of antibiotic treatment (related to Figure 4).

Groups of CBA mice (*n* = 6) were mock-infected or infected intragastrically with 1 x 10^9 CFU/animal of the virulent *S.* Typhimurium wild type (wt) or the avirulent *invA spiB* mutant (*invA spiB*) and samples were collected at the indicated time points for 16S profiling of the microbial community present in colon contents. (A) The pie graphs show the average relative abundances of phylogenetic groupings at the class level on day 17 after infection. (B and E) Normalized abundances of members of the class *Bacteroidia* (B) and members of the family *Enterobacteriaceae* (E) in colon contents at the indicated days after infection. Boxes in whisker plots represent the second and third quartiles, while lines indicate the first and fourth quartiles. (C) Weighted principal coordinate analysis of 16S profiling data. Each dot represents data from one animal. (D) The heat map indicates positive (red) and negative (blue) correlations between the average abundances of phylogenetic groupings at the class level detected at 10 and 17 days after infection.

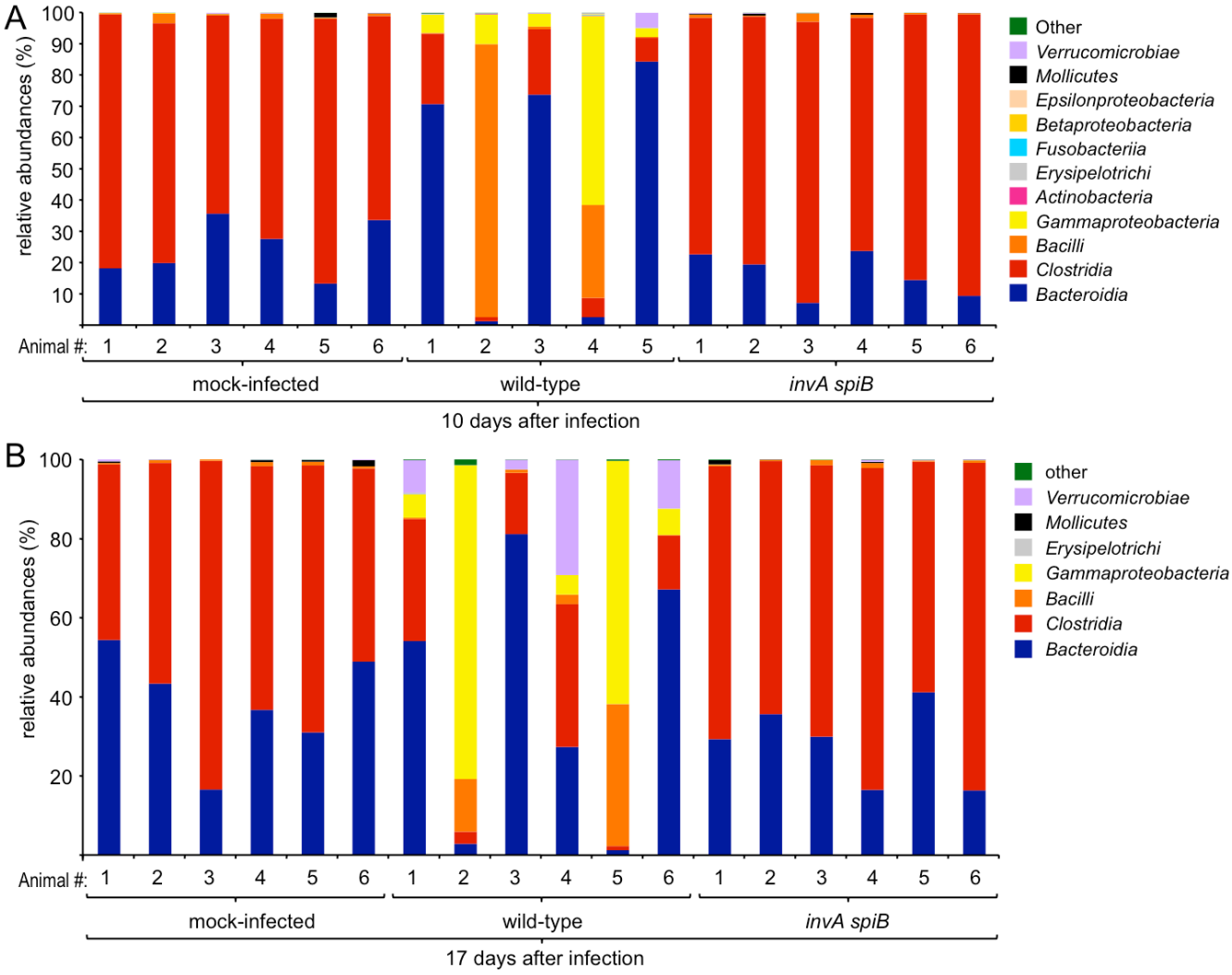

Figure S5: Relative abundances of phylogenetic groupings at the class level during *S.* Typhimurium infection (related to Figure 4).

Groups of CBA mice (*n* is indicated in each graph) were mock-infected or infected intragastrically with 1 x 10^9 CFU/animal of the virulent *S.* Typhimurium wild type (wt) or the avirulent *invA spiB* mutant (*invA spiB*) and samples were collected at the indicated time points for 16S profiling of the microbial community present in colon contents. The bar graphs show the average relative abundances of phylogenetic groupings at the class level on days 10 (A) and 17 (B) after infection for individual animals.

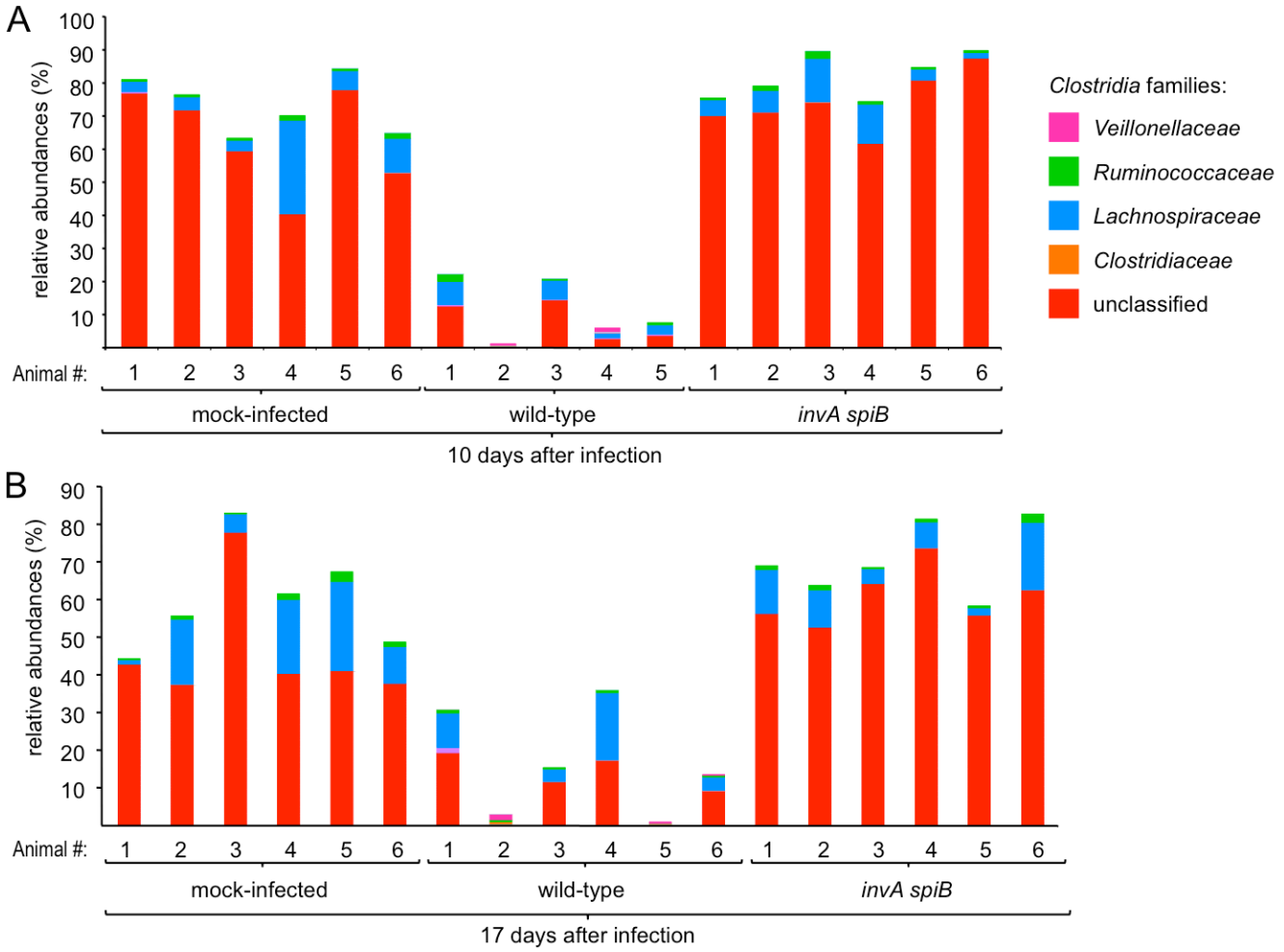

Fig. S6: Relative abundances of *Clostridia* families during *S.* Typhimurium infection (related to Figure 4).

Groups of CBA mice (*n* is indicated in each graph) were mock-infected or infected intragastrically with 1 x 10^9 CFU/animal of the virulent *S.* Typhimurium wild type (wild-type) or the avirulent *invA spiB* mutant (*invA spiB*) and samples were collected at the indicated time points for 16S profiling of the microbial community present in colon contents. The bar graphs show the average relative abundances of *Clostridia* families on days 10 (A) and 17 (B) after infection for individual animals.

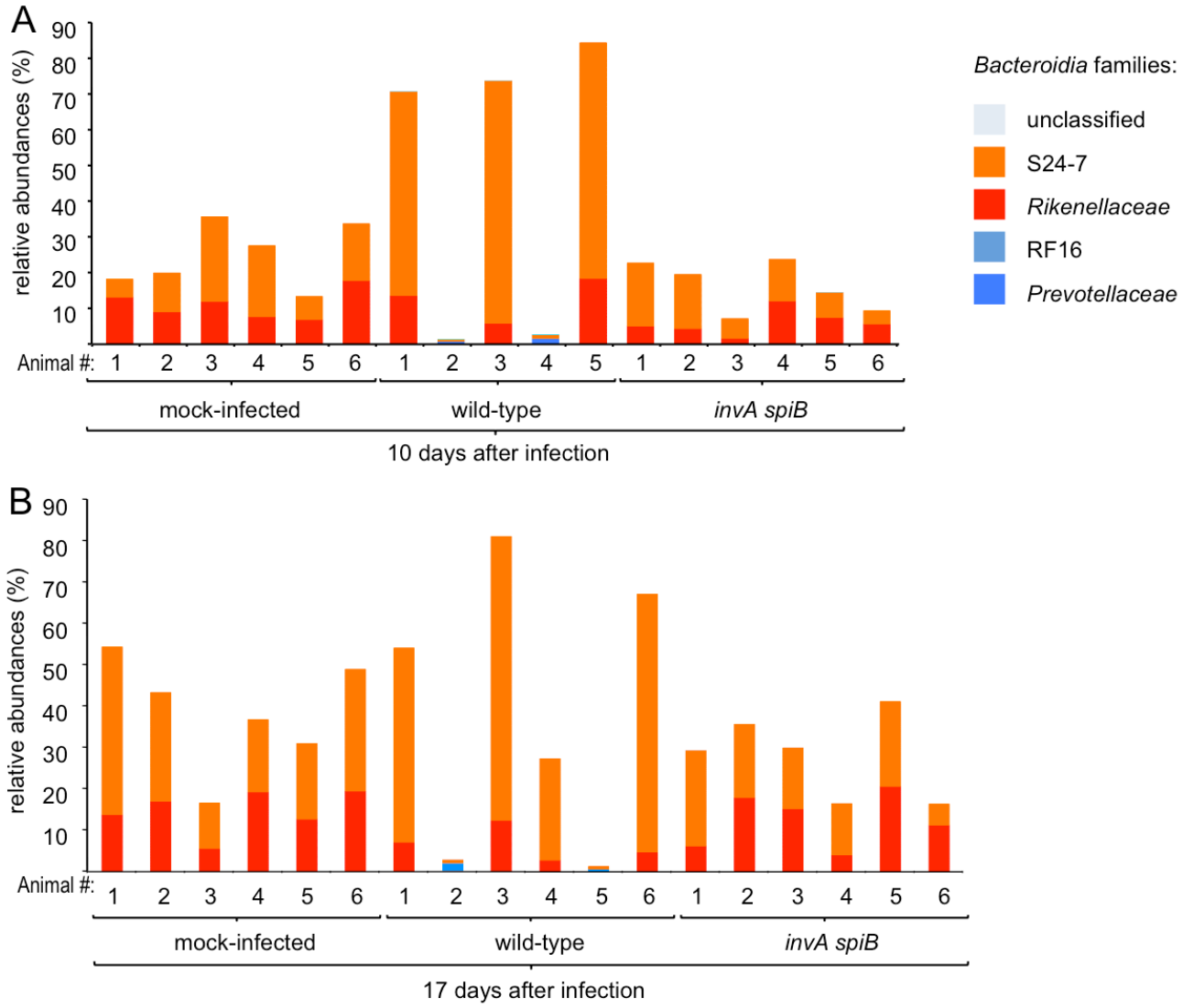

Fig. S7: Relative abundances of *Bacteroidia* families during *S.* Typhimurium infection (related to Figure 4).

Groups of CBA mice (*n* is indicated in each graph) were mock-infected or infected intragastrically with 1 x 10^9 CFU/animal of the virulent *S.* Typhimurium wild type (wild-type) or the avirulent *invA spiB* mutant (*invA spiB*) and samples were collected at the indicated time points for 16S profiling of the microbial community present in colon contents. The bar graphs show the average relative abundances of *Bacteroidia* families on days 10 (A) and 17 (B) after infection for individual animals.

SUPPLEMANTARY TABLES

Table S1: *S.* Typhimurium and *E. coli* strains used in this study (related to *Bacterial Strains and Plasmids* section in *Experimental Procedures*)

S. Typhimurium		
Strain	Genotype	Reference
IR715	Nalidixic acid-resistant derivative of ATCC 14028	(Stojiljkovic et al., 1995)
FR102	IR715 *cyxA*::pPT48 ($Carb^r$)	This Study
FR103	IR715 *cydA*::pFR9 (Cm^r)	This Study
FR104	IR715 *cyxA*::pPT48 Δ*napA* Δ*narZ narG*:: pCAL18 ($Carb^r$,Cm^r)	This Study
FR105	IR715 Δ*invA*::*tetRA* Δ*spiB*::KSAC *cyxA*:: pPT48 (Tet^r; Kan^r, $Carb^r$)*	This Study
CAL82	IR715 Δ*napA* Δ*narZ narG*::pCAL18 (Cm^r)	This Study
CAL49	IR715 Δ*napA* Δ*narZ*	This Study
CAL45	IR715 *narZ*::pCAL10 (Cm^r)	(Lopez et al., 2012)
CAL46	IR715 Δ*napA narZ*::pCAL10	(Lopez et al., 2012)
SPN452	IR715 Δ*invA*::*tetRA* Δ*spiB*::KSAC (Tet^r; Kan^r)	(Raffatellu et al., 2009)
E. coli		
Strain	Genotype	Reference
DH5α λ*pir*	F^- *endA1 hsdR17* ($r^- m^+$) *supE44 thi-1 recA1 gyrA96 relA1* Δ(*lacZYA-argF*)U169 *deoR nupG* ϕ80*lacZ*ΔM15 λ*pir*	(Pal et al., 2005)
S17-1 λ*pir*	*zxx*::RP4-2-Tet^r::Mu-Kan^r::Tn*7 recA1 thi*	(Simon et al., 1983)

	pro hsdR ($r^- m^+$) λ*pir*	
TOP10	F^- *mcrA* Δ(*mrr-hsdRMS-mcrBC*) ϕ80*lacZ*ΔM15 *lacX74 recA1 araD139* Δ(*ara - leu*)*7697 galE15 galK rpsL endA1 nupG*	Invitrogen

*Cm^r: chloramphenicol resistance; $Carb^r$: carbenicillin resistance; Kan^r: kanamycin resistance

Table S2: Plasmids used in this study (related to *Bacterial Strains and Plasmids* section in *Experimental Procedures*)

Designation	Relevant Characteristics	Reference/source
pCR2.1	Cloning vector	Invitrogen
pGP704	*ori*(R6K) *mobRP4* ($Carb^r$)	(Miller and Mekalanos, 1988)
pEP185.2	*ori*(R6K) *mobRP4* (Cm^r)	(Kinder et al., 1993)
pRDH10	sacRB *ori*(R6K) *mobRP4* (Tet^r Cm^r)	(Kingsley et al., 1999)
pPT48	*'cyxA'* gene fragment cloned into pGP704; insertion of pPT48 into the IR715 chromosome *cyxA* gene.	This Study
pFR9	*'cydA'* gene fragment cloned into pEP185.2; insertion of pFR9 into the IR715 chromosome *cydA* gene.	This Study
pCAL18	*'narG'* gene fragment from pCAL5 cloned into pEP185.2; insertion of pCAL18 into the IR715 chromosome disrupts *narG*.	This Study
pCAL5	*'narG'* gene fragment cloned into pGP704	(Lopez et al., 2012)
pCAL10	Upstream and downstream regions of *'narZ'* cloned into pRDH10	(Lopez et al., 2012)

Table S3: Primers used in this study (related to *Bacterial Strains and Plasmids* section in *Experimental Procedures*)

Target gene / organism	Sequence	Reference
cyxA / *S.* Typhimurium	5'-GGTACCCTTACCAGTTCGGAAC-3' 5'-GATATCGCCTACCAGCGTAAG-3'	This study
cydA / *S.* Typhimurium	5'- CTGCAGCCCGGGGGATCCACT AGTTGCGATGTTCATCCTCGGT-3' 5'- GAGCTCCACCGCGGTGGCGGC CGCTGATCTGAATCGCCAGATG-3'	This study
Gapdh / *Mus musculus*	5'-TGTAGACCATGTAGTTGAGGTCA-3' 5'-AGGTCGGTGTGAACGGATTTG-3'	(Godinez et al., 2008)
Kc / *Mus musculus*	5'-TGCACCCAAACCGAAGTCAT-3' 5'-TTGTCAGAAGCCAGCGTTCAC-3'	(Godinez et al., 2008)
Mip2 / *Mus musculus*	5'-AGTGAACTGCGCTGTCAATGC-3' 5'-AGGCAAACTTTTTGACCGCC-3'	(Godinez et al., 2008)
16S rRNA gene from members of the class *Clostridia*	5'-ACTCCTACGGGAGGCAGC-3' 5'-GCTTCTTTAGTCAGGTACCGTCAT-3'	(Croswell et al., 2009)

Table S4: Criteria for blinded scoring of histopathological changes (related to Figure 3B)

Score	Submucosal edema	Epithelial damage	Exudate	Infiltration by PMNs[a,b]	Mononuclear cell infiltration[a]
0	No changes	No changes	No changes	No changes (0-5)	No changes (0)
1	Detectable (<10%)	Desquamation	Slight accumulation	6-20	5-10
2	Mild (10%-20%)	Mild erosion	Mild accumulation	21-60	10-20
3	Moderate (20%-40%)	Marked erosion	Moderate accumulation	60-100	20-40
4	Marked (>40%)	Ulceration	Marked accumulation	>100	>40

[a] Number of cells per high power field (400x)
[b] PMN, polymorphonuclear cells

SUPPLEMENTAL EXPERIMENTAL PROCEDURES

Bacterial culture conditions

Unless indicated otherwise, *S.* Typhimurium and *E. coli* strains were routinely grown aerobically at 37°C in LB broth (BD Biosciences) or on LB plates. Antibiotics were added to the media at the following concentrations: 0.03 mg/ml chloramphenicol, 0.1 mg/ml carbenicillin, 0.05 mg/ml kanamycin, and 0.05 mg/ml nalidixic acid. For growth under different microaerobic or anaerobic conditions, minimal medium containing glycerol as the sole carbon source was inoculated with the indicated strain mixtures and incubated at 37°C either in a hypoxia chamber (set at 8% or 0.8% oxygen) or in an anaerobe chamber (0% oxygen).

Spore preparations

Spores were isolated from cecal contents of mice as described previously (Momose et al., 2009), with some modifications. Briefly, cecal contents from C57BL/6 mice were diluted 1:10 in PBS and chloroform was added to a final concentration of 3%. The mixture was incubated in a 37°C shaker for at least 30 minutes. The chloroform was allowed to settle to the bottom of the tube and the top layer containing spores was collected into a new tube.

Construction of plasmids

PCR products were cloned into vectors using Gibson Assembly (New England Biolabs, Ipswich, MA) or cloned into pCR2.1 using the TOPO TA cloning kit (Invitrogen, Carlsbad) and sequenced (SeqWright Fisher Scientific, Houston) prior to subcloning into the appropriate vectors.

An internal fragment of the *cyxA* gene was amplified by PCR using the primers listed in Table S3. The *cyxA* PCR product was then cloned into pGP704 using the KpnI and EcorV restriction enzyme sites to construct pPT48. A fragment of the *cydA* gene was amplified by PCR and cloned into pEP185.2 using Gibson Assembly to create pFR9. An internal fragment of the *narG* gene from pCAL5 was cloned into pEP185.2 using the SacI and XbaI restriction enzyme sites creating pCAL18.

To generate plasmids that served as standards for real-time PCR, primer sets (Table S3) were used in a standard PCR reaction to amplify the respective target genes, which were subsequently inserted into pCR2.1 using the TOPO cloning kit (Life Technologies). The resulting plasmids were sequenced to ensure accuracy.

Generalized Phage Transduction

Phage P22 HT *int-105* was used for generalized transduction. Transductants were routinely purified from phage contamination on Evans blue-Uranine agar and then cross-struck against P22 H5 to confirm phage sensitivity.

Using phage transduction, the *cyxA*::pPT48 mutation from FR102 was introduced into CAL82 and SPN452 to yield strains FR104 and FR105, respectively.

Construction of *S.* Typhimurium mutants

Suicide plasmids were propagated in *E. coli* DH5α λ*pir* and introduced into the *S.* Typhimurium strain IR715 by conjugation using *E. coli* S17-1 λ*pir* as a donor strain. Exconjugants were selected on LB agar plates containing nalidixic acid and antibiotics selecting for integration of the suicide plasmid. Integration of the plasmids in the correct location on the chromosome was verified by PCR. Using this methodology, pPT48 and pFR9 were integrated into the *cyxA* and *cydA* genes of IR715 to yield strains FR102 and FR103, respectively.

The *narZ*::pCAL10 mutation from CAL45 was introduced into CAL46 and sucrose counter-selection was performed as described previously (Kingsley et al., 1999) to remove the Cm^r marker. A strain that was sucrose-tolerant and Cm^s was verified by PCR and designated CAL49.

pCAL18 was integrated into the *narG* gene of strain CAL49 to yield CAL82.

Animal Experiments

C57BL/6 mice were treated with 20 mg/animal streptomycin or mock-treated and orally inoculated 24 hours later with 0.1 ml sterile LB broth (mock infection), with an equal mixture of 5 x 10^8

CFU of each *S*. Typhimurium strain in 0.1 ml LB broth or with 5 x 10^8 CFU of individual *S*. Typhimurium strains. After euthanasia, organs were collected for RNA purification and bacteriological analysis. For competitive infections, the ratio of recovered bacterial strains (output ratio) was divided by the ratio present in the inoculum (input ratio) to determine the competitive index (CI). For treatment of infected C57BL/6 mice with a community of 17 *Clostridia* strains or with spore preparations, animals were treated with 20 mg/animal streptomycin and orally inoculated 24 hours later with *S*. Typhimurium. One-day after infection, mice were inoculated with 0.2 ml of spores or with 17 human Clostridia isolates by oral gavage.

CBA mice were inoculated with 0.1 ml of a suspension (LB broth) containing an equal mixture of 5×10^7 CFU of each bacterial strain. For single strain infections, animals were inoculated with approximately 1 x 10^8 CFU per animal or 1 x 10^9 CFU per animal. For treatment of CBA mice with a mixture of 17 *Clostridia* strains, animals were infected with *S.* Typhimurium strains and 5, 7 and 10 days after infection mice were inoculated with 0.2 ml of a culture of 17 human Clostridia isolates by oral gavage.

For transmission studies, mice from the same cage were split into two new cages (two mice per cage). Two mice were mock-treated and the other two mice (donors) were infected with 1 x 10^8 CFU of the indicated *S*. Typhimurium strain. Ten days after infection, two mock-treated mice (recipients) were co-housed with two infected mice. Feces were collected after 7 days of co-housing for bacterial enumeration. Colon contents were collected after 18 days of co-housing. Successful "transmission" was defined as recipient mice harboring detectable levels of *S*. Typhimurium in their feces at one of the indicated time points.

Microbiota analysis

Bacterial DNA was amplified via a PCR enrichment of the 16S rRNA gene (V4 region) using primers 515F (5′-GTGCCAGCMGCCGCGGTAA-3′) and 806R (5′-GGACTACHVGGGTWTCTAAT-3′) modified by addition of barcodes for multiplexing. Libraries were sequenced with an Illumina MiSeq system. Sample sequences were demultiplexed and trimmed, followed by filtering for quality. QIIME

open-source software (http://qiime.org) (Caporaso et al., 2010) was used for initial identification of operational taxonomic units (OTU), clustering, and phylogenetic analysis. Principal Coordinate (PC) analysis taxa summaries using weighted UniFrac were created through QIIME. Samples containing less than 1000 quality reads were removed from dataset. Subsequent data transformation was performed using MEGAN 4 software (http://ab.inf.uni-tuebingen.de/software/megan4/) (Huson and Weber, 2013) and then further analyzed using Explicit (http://www.explicet.org/) (Robertson et al., 2013) and METAGENassist (http://www.metagenassist.ca/) (Arndt et al., 2012). Data are available at the NCBI BioSample database: SAMN04543794, SAMN04543795, SAMN04543796, SAMN04543797, SAMN04543798, SAMN04543799, SAMN04543800, SAMN04543801, SAMN04543802, SAMN04543803, SAMN04543804, SAMN04543805, SAMN04543806, SAMN04543807, SAMN04543808, SAMN04543809, SAMN04543810, SAMN04543811, SAMN04543812, SAMN04543813, SAMN04543814, SAMN04543815, SAMN04543816, SAMN04543817, SAMN04543818, SAMN04543819, SAMN04543820, SAMN04543821, SAMN04543822, SAMN04543823, SAMN04543824, SAMN04543825, SAMN04543826, SAMN04543827, SAMN04543828.

Hypoxia Staining

Colon and cecal samples were fixed in 10% buffered formalin phosphate and paraffin-embedded tissue was probed with mouse anti-pimonidazole monoclonal IgG1 (MAb1 4.3.11.3) and then stained with Cy-3 conjugated goat anti-mouse antibody (Jackson Immuno Research Laboratories). Samples were counterstained with DAPI using SlowFade Gold mountant.

Histopathology

Formalin fixed cecal tissue sections were stained with hematoxylin and eosin, and a veterinary pathologist performed a blinded evaluation using criteria shown in Table S4 as described previously (Spees et al., 2013). Representative images were obtained using an Olympus BX41 microscope and the brightness adjusted (Adobe Photoshop CS2).

RNA isolation

For murine RNA isolation, colon tissue sections were homogenized in a Mini-Beadbeater (BioSpec Products, Bartlesville, OK) and RNA was isolated by the TRI-Reagent method (Molecular Research Center, Inc.) following the manufacturer's protocol. Contaminating DNA was removed using the DNA-free kit (Applied Biosystems) and RNA was stored at -80°C.

Measurements of short-chain fatty acid concentrations

Samples of cecal and colon contents were diluted with 80% ethanol (10 µl/mg) and gently agitated overnight at 4°C. The homogenized samples were centrifuged at 21,000 x g for 5 min. 200 µl of the supernatants were transferred centrifuged at 21,000 x g again for 20 min. For each sample, 20 µl of the supernatant was mixed with 20 µl of 200 mM N-(3-Dimethylaminopropyl)-N′-ethylcarbodiimide hydrochloride (1-EDC HCl) (SIGMA) in 5% pyridine (SIGMA) and 40 uL of 100 mM 2-Nitrophenylhydrazine (2-NPH) (SIGMA) in 80% acetonitrile (ACN) (SIGMA) with 50 mM HCl. The mixture was incubated at 40°C for 30 min. After reacting, 400 µl of 10% ACN was added to the solution. Then 1 µl the solution was injected into an Agilent 6490 triple quadruple mass spectrometer for analysis.

REFERENCES FOR SUPPLEMENTAL MATERIALS

Arndt, D., Xia, J., Liu, Y., Zhou, Y., Guo, A.C., Cruz, J.A., Sinelnikov, I., Budwill, K., Nesbo, C.L., and Wishart, D.S. (2012). METAGENassist: a comprehensive web server for comparative metagenomics. Nucleic Acids Res *40*, W88-95.

Caporaso, J.G., Kuczynski, J., Stombaugh, J., Bittinger, K., Bushman, F.D., Costello, E.K., Fierer, N., Pena, A.G., Goodrich, J.K., Gordon, J.I.*, et al.* (2010). QIIME allows analysis of high-throughput community sequencing data. Nat Methods *7*, 335-336.

Croswell, A., Amir, E., Teggatz, P., Barman, M., and Salzman, N.H. (2009). Prolonged impact of antibiotics on intestinal microbial ecology and susceptibility to enteric Salmonella infection. Infection and immunity *77*, 2741-2753.

Godinez, I., Haneda, T., Raffatellu, M., George, M.D., Paixao, T.A., Rolan, H.G., Santos, R.L., Dandekar, S., Tsolis, R.M., and Bäumler, A.J. (2008). T cells help to amplify inflammatory responses induced by Salmonella enterica serotype Typhimurium in the intestinal mucosa. Infection and immunity *76*, 2008-2017.

Huson, D.H., and Weber, N. (2013). Microbial community analysis using MEGAN. Methods Enzymol *531*, 465-485.

Kinder, S.A., Badger, J.L., Bryant, G.O., Pepe, J.C., and Miller, V.L. (1993). Cloning of the YenI restriction endonuclease and methyltransferase from Yersinia enterocolitica serotype O8 and construction of a transformable R-M+ mutant. Gene *136*, 271-275.

Kingsley, R.A., Reissbrodt, R., Rabsch, W., Ketley, J.M., Tsolis, R.M., Everest, P., Dougan, G., Bäumler, A.J., Roberts, M., and Williams, P.H. (1999). Ferrioxamine-mediated Iron(III) utilization by Salmonella enterica. Appl Environ Microbiol *65*, 1610-1618.

Lopez, C.A., Winter, S.E., Rivera-Chavez, F., Xavier, M.N., Poon, V., Nuccio, S.P., Tsolis, R.M., and Bäumler, A.J. (2012). Phage-mediated acquisition of a type III secreted effector protein boosts growth of salmonella by nitrate respiration. mBio *3*.

Miller, V.L., and Mekalanos, J.J. (1988). A novel suicide vector and its use in construction of insertion mutations: osmoregulation of outer membrane proteins and virulence determinants in Vibrio cholerae requires toxR. Journal of bacteriology *170*, 2575-2583.

Momose, Y., Maruyama, A., Iwasaki, T., Miyamoto, Y., and Itoh, K. (2009). 16S rRNA gene sequence-based analysis of clostridia related to conversion of germfree mice to the normal state. J Appl Microbiol *107*, 2088-2097.

Pal, D., Venkova-Canova, T., Srivastava, P., and Chattoraj, D.K. (2005). Multipartite regulation of rctB, the replication initiator gene of Vibrio cholerae chromosome II. Journal of bacteriology *187*, 7167-7175.

Raffatellu, M., George, M.D., Akiyama, Y., Hornsby, M.J., Nuccio, S.P., Paixao, T.A., Butler, B.P., Chu, H., Santos, R.L., Berger, T.*, et al.* (2009). Lipocalin-2 resistance confers an advantage to Salmonella enterica serotype Typhimurium for growth and survival in the inflamed intestine. Cell Host Microbe *5*, 476-486.

Robertson, C.E., Harris, J.K., Wagner, B.D., Granger, D., Browne, K., Tatem, B., Feazel, L.M., Park, K., Pace, N.R., and Frank, D.N. (2013). Explicet: graphical user interface software for metadata-driven management, analysis and visualization of microbiome data. Bioinformatics *29*, 3100-3101.

Simon, R., Priefer, U., and Puhler, A. (1983). A Broad Host Range Mobilization System for In Vivo Genetic Engineering: Transposon Mutagenesis in Gram Negative Bacteria. Nat Biotech *1*, 784-791.

Spees, A.M., Wangdi, T., Lopez, C.A., Kingsbury, D.D., Xavier, M.N., Winter, S.E., Tsolis, R.M., and Bäumler, A.J. (2013). Streptomycin-Induced Inflammation Enhances Escherichia coli Gut Colonization Through Nitrate Respiration. mBio *4*, e00430-00413.

Stojiljkovic, I., Bäumler, A.J., and Heffron, F. (1995). Ethanolamine utilization in Salmonella typhimurium: nucleotide sequence, protein expression, and mutational analysis of the cchA cchB eutE eutJ eutG eutH gene cluster. Journal of bacteriology *177*, 1357-1366.